LMU LUDWIG-MAXIMILIANS-UNIVERSITÄT MÜNCHEN

Molecular Recognition

Chemical Understanding of Biological Complexity

Dr. Henry Dube

Supramolecular Chemistry

Covalent **Noncovalent**

Atoms → ***Molecules*** → ***Supramolecules***

Synthesis

Molecular Interactions
Molecular Assembly
Molecular Recognition

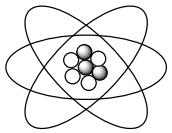

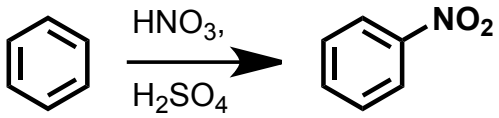

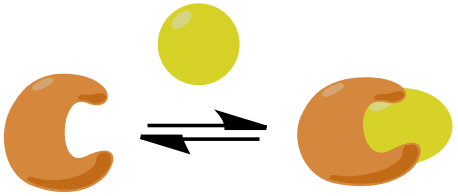

From Making Substrates to Making Receptors

Chemical Substrate

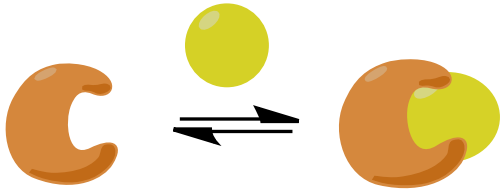

Natural Receptor

Drug Design

Substrate

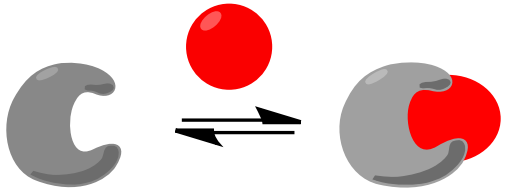

Synthetic Receptor

Supramolecular Chemistry

Making Substrates: Structure Based Drug Design

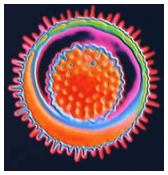

Disease

Structure determination

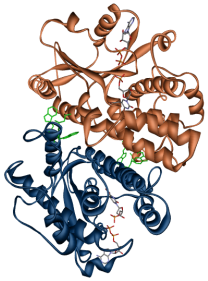

Target
X-Ray Crystal structure

Ligand Design

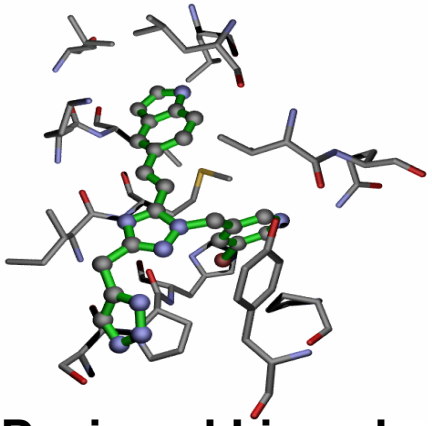

Designed Ligand

Synthesis

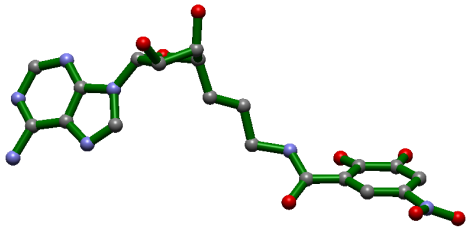

Synthesized Ligand

Assay

Clinical Studies, Drugs

Compound	R	IC_{50} [nM]	ΔG_{inh} [kJ mol^{-1}]	σ_p	pK_a
1a	NO_2	9	-47.8	0.78	4.42
1b		21	-45.6	0.06	6.87
1c		23	-45.3	-0.03	7.06
1d		23	-45.3	0.23	6.89
1e		27	-44.9	–	6.15
1f	Br	28	-44.8	0.23	6.54
1g		29	-44.7	0.29	6.18
1h	CN	29	-44.7	0.66	5.18
1i		34	-44.3	0.43	5.42
1j	CF_3	35	-44.3	0.54	6.22

Compound	R	IC_{50} [nM]	ΔG_{inh} [kJ mol^{-1}]	σ_p	pK_a
1k		39	-44.0	0.80	5.74
1l		42	-43.8	–	6.95
1m	Cl	44	-43.7	0.23	6.65
1n		83	-42.0	–	5.46
1o		97	-41.6	0.05	6.34
1p		213	-39.6	–	5.07
1q		608	-36.9	-0.09	7.56
1r		1370	-34.8	-0.15	7.63
1s		2000	-33.8	0.36	6.25
1t	H	2600	-33.1	0	7.37

Biologically active molecules

From Making Substrates to Making Receptors

Chemical Substrate

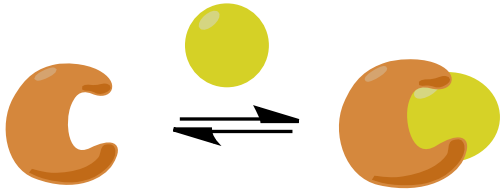

Natural Receptor

Drug Design

Substrate

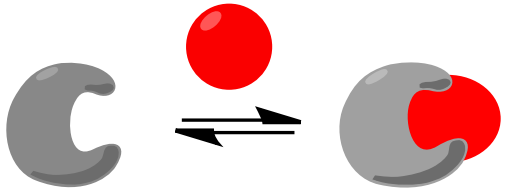

Synthetic Receptor

Supramolecular Chemistry

Early Supramolecular Chemistry

1967 Pedersen **1978** Lehn **1953** Freudenberg, Cramer, Plieninger

Complexation of Cations

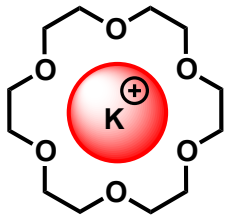

Crown ether

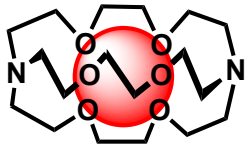

Cryptand

Complexation of Neutral Molecules

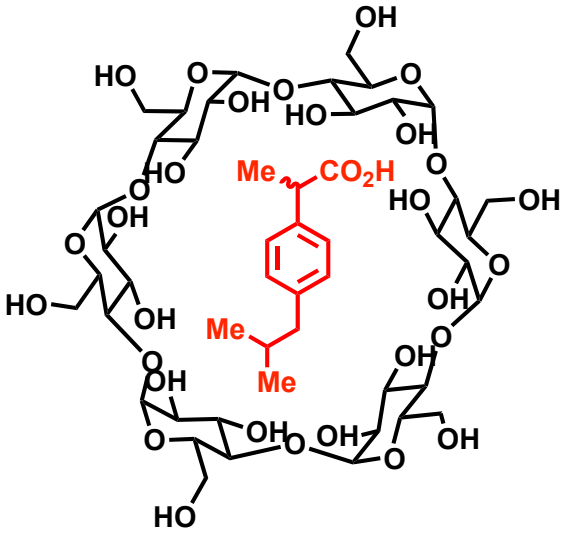

α-Cyclodextrin

Lehn, *Angew. Chem.* **1988**, *100*, 91.
Cram, *Angew. Chem.* **1988**, *100*, 1041.
Pedersen, *Angew. Chem.* **1988**, *100*, 1053.

Molecular Capsules

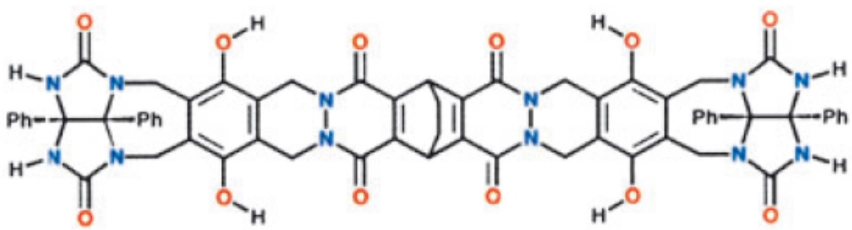

Wyler, de Mendoza, Rebek, Jr., *Angew. Chem. Int. Ed.* **1993**, *32*, 1699.
Kang, Rebek, Jr., *Nature* **1996**, *382*, 239.

Molecular Recognition: Biomimetic Chemistry

Synthetic Model for Hemoglobin and Myoglobin

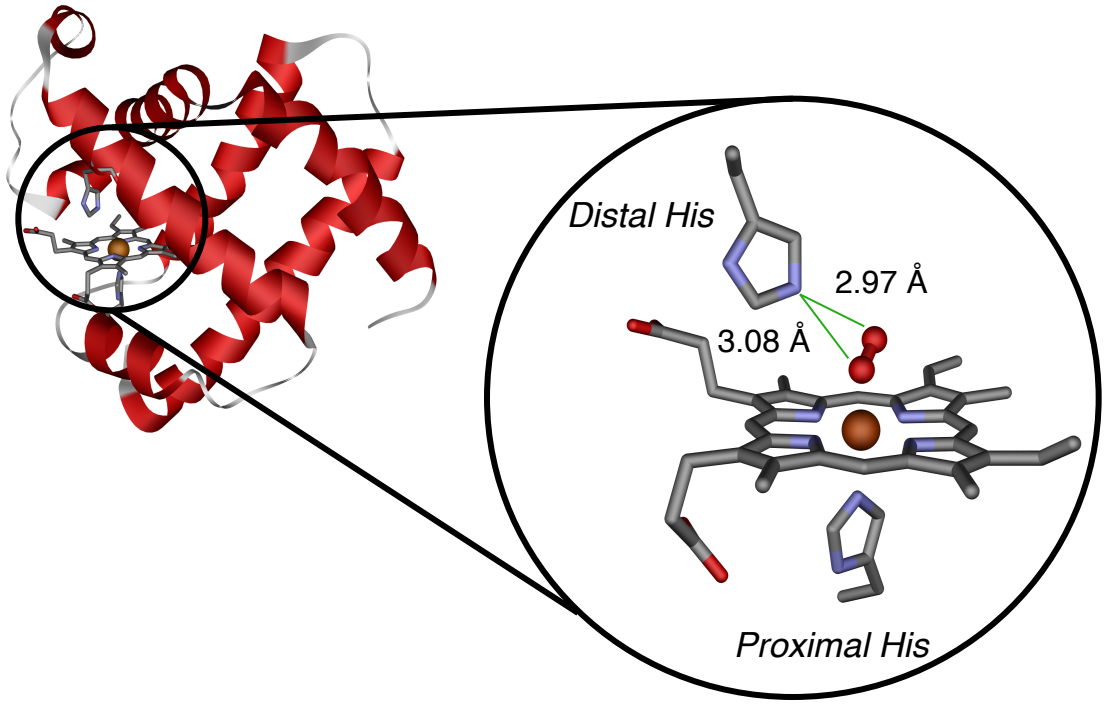

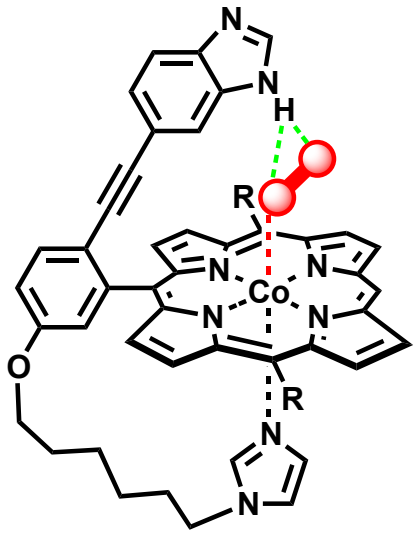

Dube, Kasumaj, Calle, Saito, Jeschke, Diederich, *Angew. Chem. Int. Ed.* **2008**, *47*, 2600.
Dube, Kasumaj, Calle, Felber, Saito, Jeschke, Diederich, *Chem. Eur. J.* **2009**, *15*, 125.

Supramolecular Chemistry: Generating Complexity

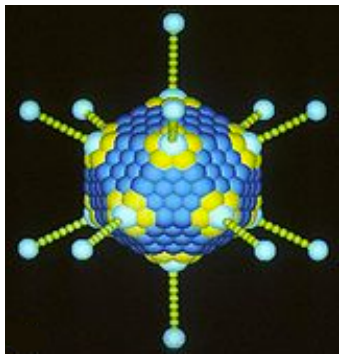

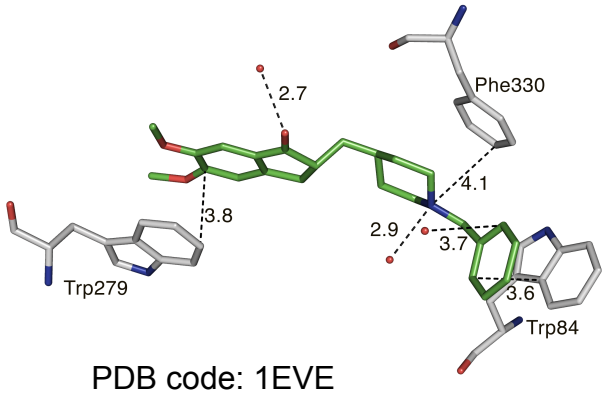

PDB code: 1EVE

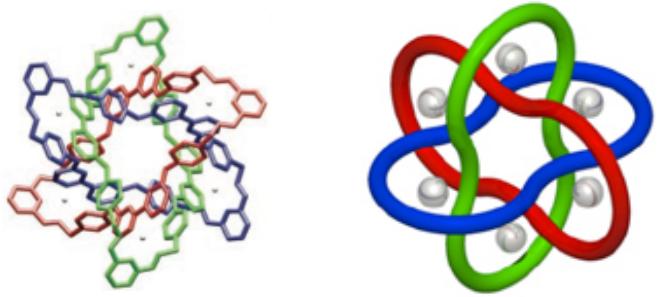

Stoddart and co-workers, *Science* **2004**, *304*, 1308

- Biology
- Drug discovery - Drug design
- Supramolecular Architectures
- Smart Materials
- Molecular Machines
- ...

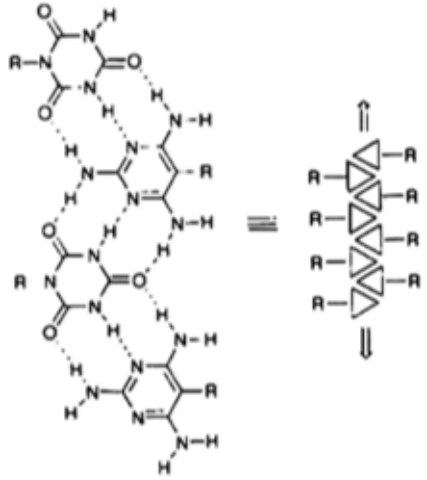

J.-M. Lehn and co-workers, *Mol. Cryst. Liq. Cryst.* **2007**, *468*, 187

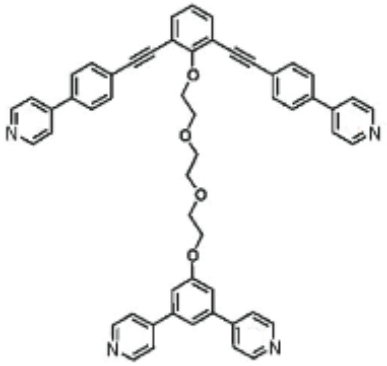

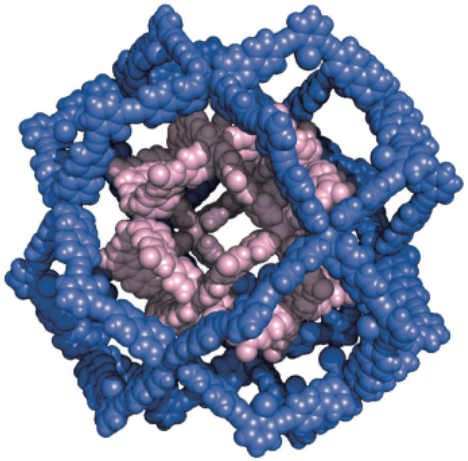

Fujita and co-workers, *Angew. Chem. Int. Ed.* **2011**, *44*, 10318

Analysis of Binding – Binding Energy

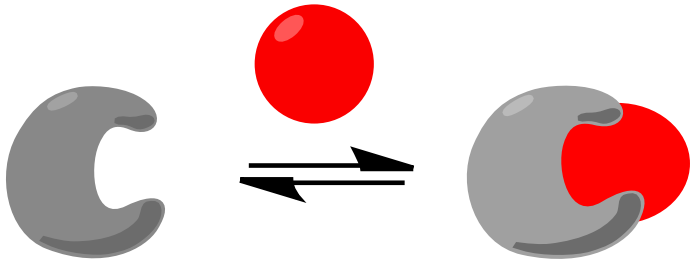

$-\Delta G$ = Binding Energy

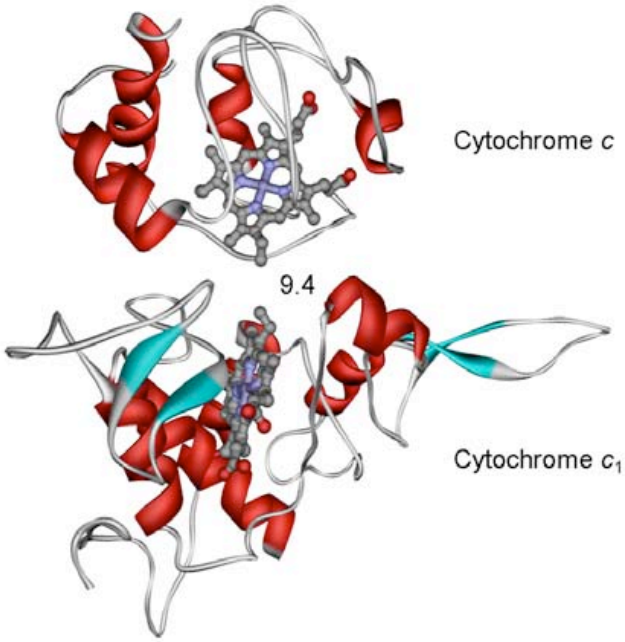

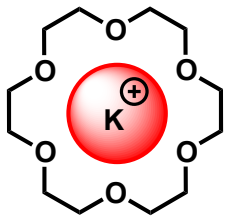

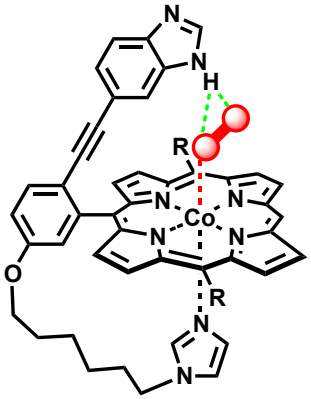

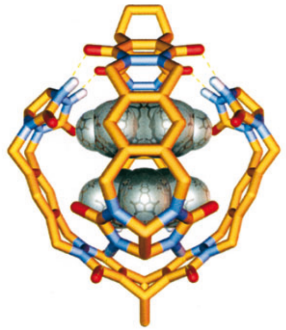

Binding Energy and Binding Constant

$-\Delta G = R \cdot T \cdot \ln K$

$-\Delta G$ = Binding Energy

K = Binding Constant

K = Complexed / Uncomplexed

–5,7 kJ/mol → K = 10 → 90.1% Complexed (if conc. = 1)

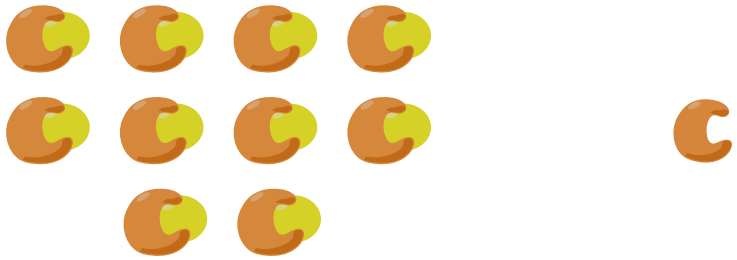

Binding Energy and Binding Constant

$-\Delta G = R \cdot T \cdot \ln K$

$-\Delta G$ = Binding Energy

K = Binding Constant

K = Complexed / Uncomplexed

–50 kJ/mol → $K = 10^9$ → 99.9999% Complexed - Nanomolar Binding

Intermolecular Interactions Are Dynamic

85 kJ/mol → Available at 25 °C

1 min

Eyring Equation: $k = k_B T/h * e^{-\Delta G/RT}$

Half Life = ln2/k

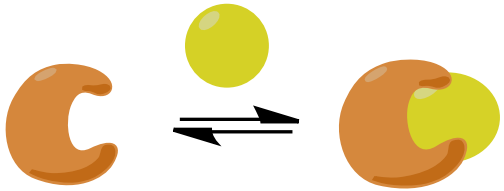

Dynamic Processes

Unless: **–85 kJ/mol → *K* = 10^{15} Femtomolar Binding**

Intermolecular Interactions Are Dynamic

Reversible Binding:

–34 kJ/mol → *K* = 10^6 → mikromolar Binding

Example: Kinase A Binding to ATP

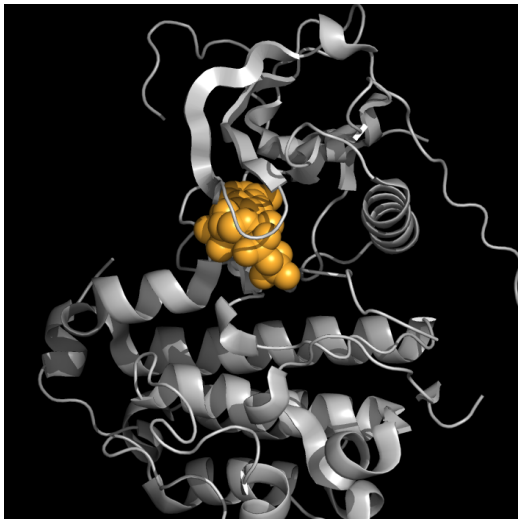

Limit to Irreversible Binding:

–68 kJ/mol → *K* = 10^{12} → picomolar Binding

Example: G Protein Binding to GTP/GDP

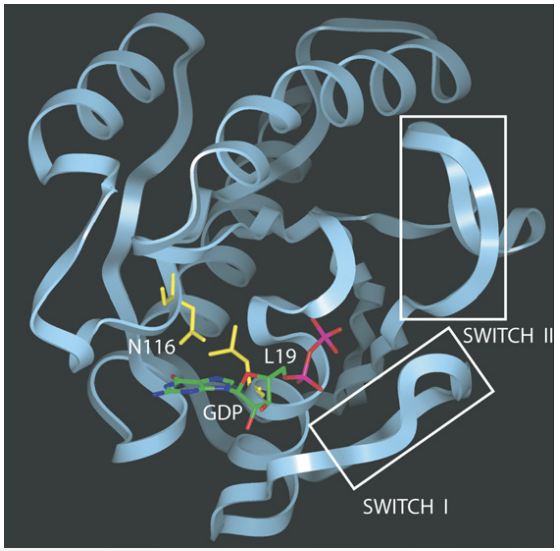

Binding Constant: What's In It? - Not so Easy

Binding in Water

$-\Delta G = -\Delta H + T\Delta S$

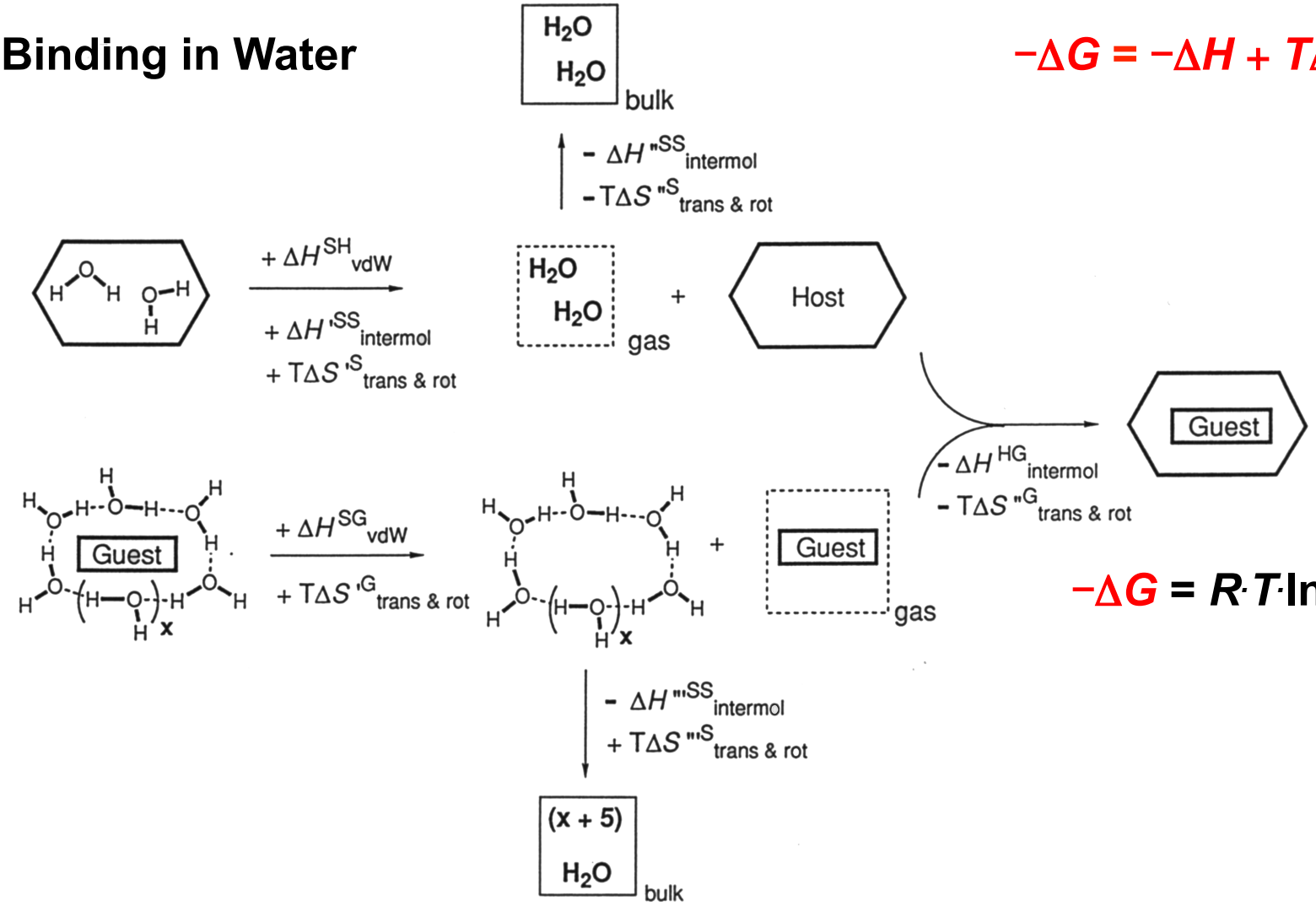

$-\Delta G = R \cdot T \cdot \ln K$

Methods to Quantify Binding

K_a, ΔG^o	ion conductivity, UV/Vis absorption, fluorescence, NMR, calorimetry.
ΔH^o, $T\Delta S^o$	Variable temperature ^{1}H NMR, van't Hoff analysis Titration microcalorimetry
ΔC_p^o	Titration microcalorimetry (heat capacity changes = $\partial(\Delta H^o)/\partial T$)

Note that $K_d \approx K_i = 1/K_a$ (supramolecular chemists use K_a, medicinal chemists K_d and K_i)

Methods to Quantify Binding

Formation of 1:1 host (H) – guest (G) complex proceeds according to:

Guest concentration

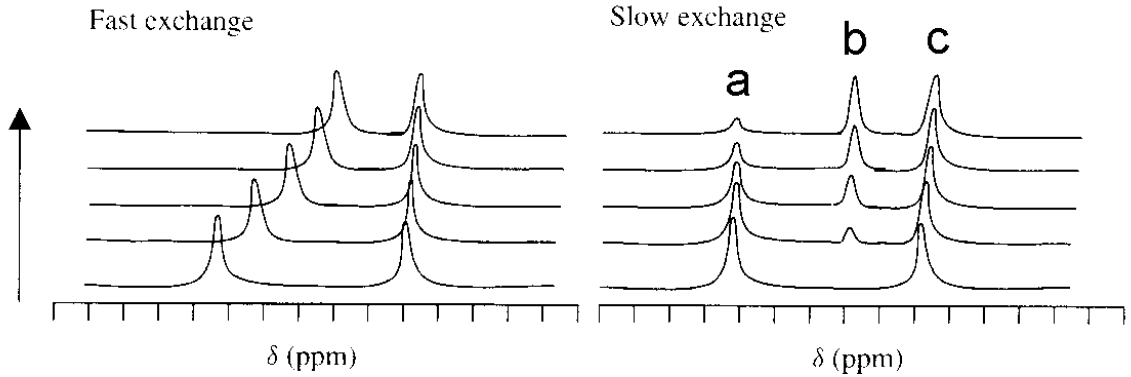

a – sensitive nucleus on free ligand

b – analogous nucleus in complex

c – nucleus insensitive to compexation

NMR titration plot for a fast equilibrating (on the NMR timescale) system

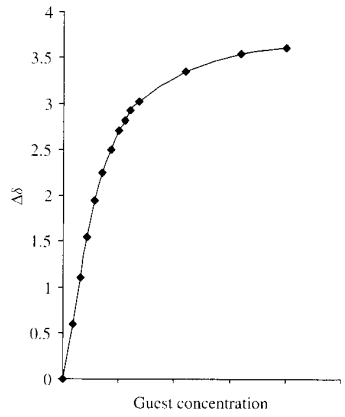

Job plot showing a 1:1 host – guest complex

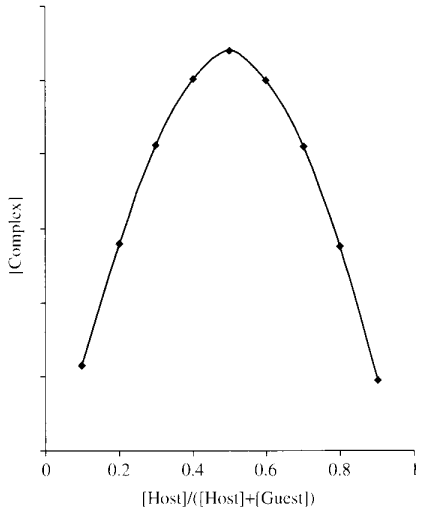

Specifics of Binding

Specific Molecular Interactions – Molecular Recognition

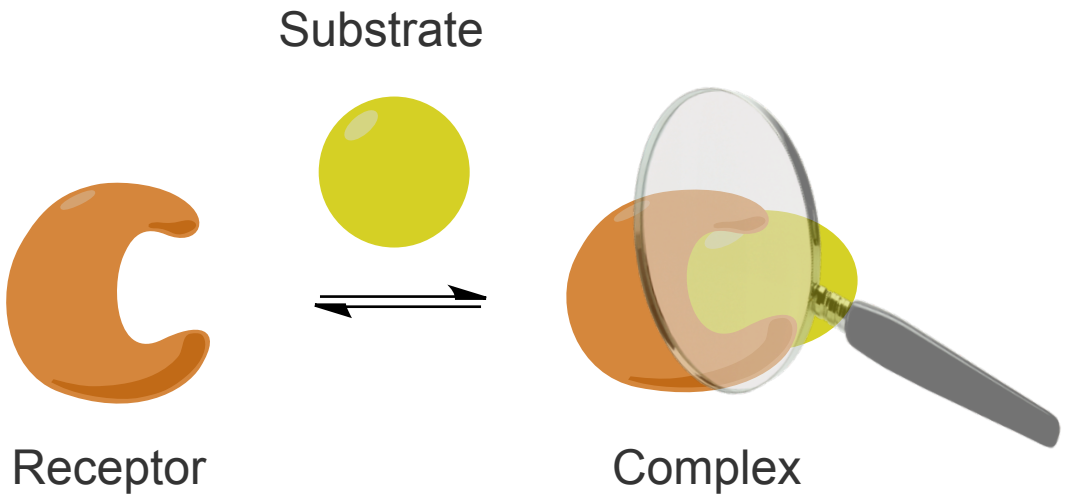

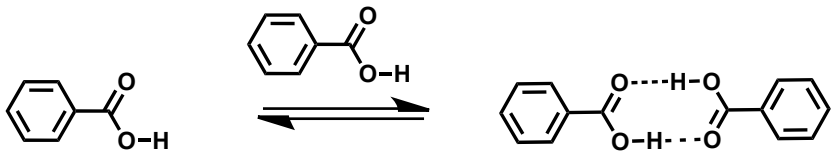

Molecular Recognition – Lock and Key

„To use a picture I would like to say that enzyme and glucoside have to fit together like *lock and key* in order to exert a chemical effect on each other.“

Fischer, *Ber. Dtsch. Chem. Ges.* **1894**, *27*, 2985.

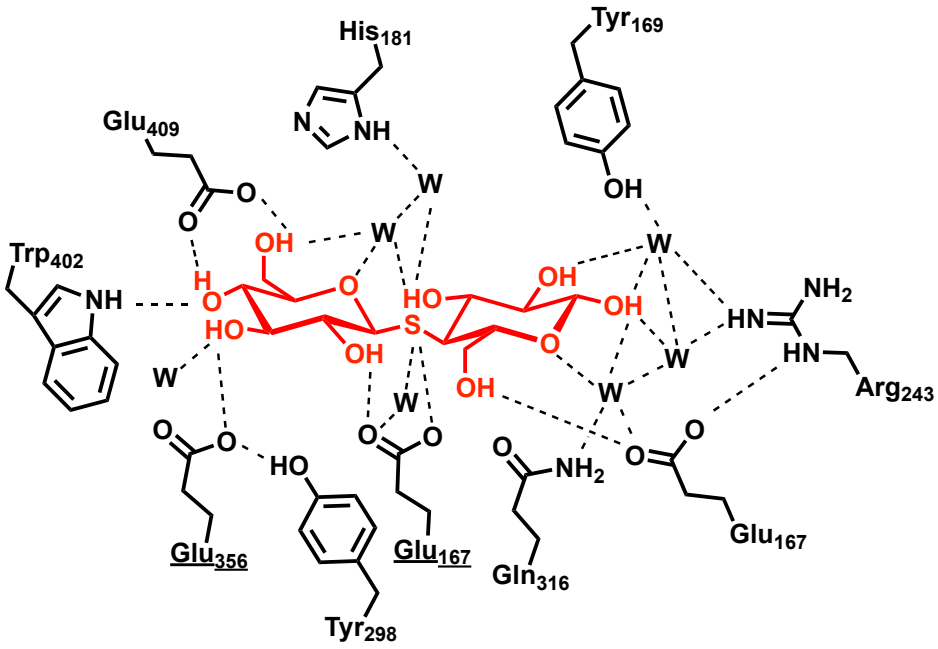

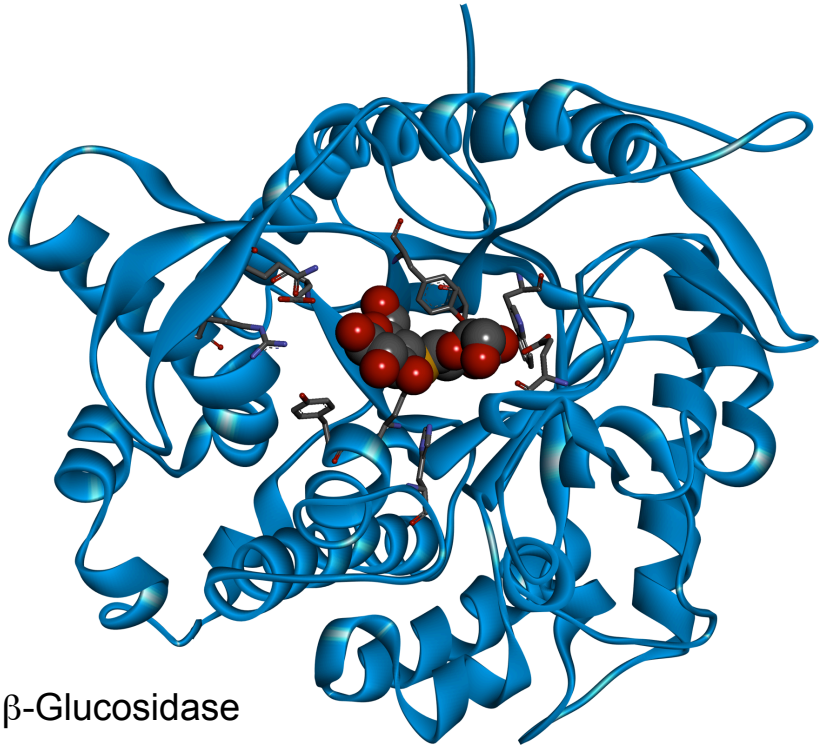

β-Glucosidase

Isorna, Polaina, Latorre-Garcia, Cañada, Gonzalez, Sanz-Aparicio, *J. Mol. Biol.* **2007**, *371*, 1204.

Molecular Recognition – Specific Interactions

Complex Network of Weak Interactions

Aricept® in Acetylcholinesterase – Alzheimer's Disease

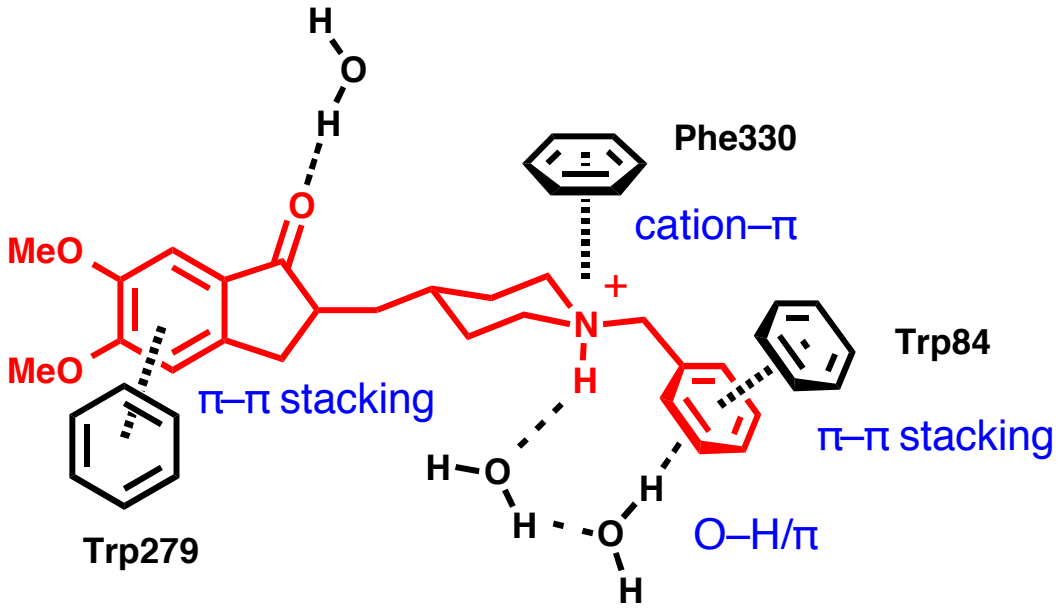

Kryger, Silman, Sussman, *J. Physiol. (Paris)* **1998**, *92*, 191–194;
Kryger, Silman, Sussman, *Structure* **1999**, *7*, 297–307.

Weak Interactions: Toolbox to Make Supramolecules

Chemical Bonds - from strong to very weak

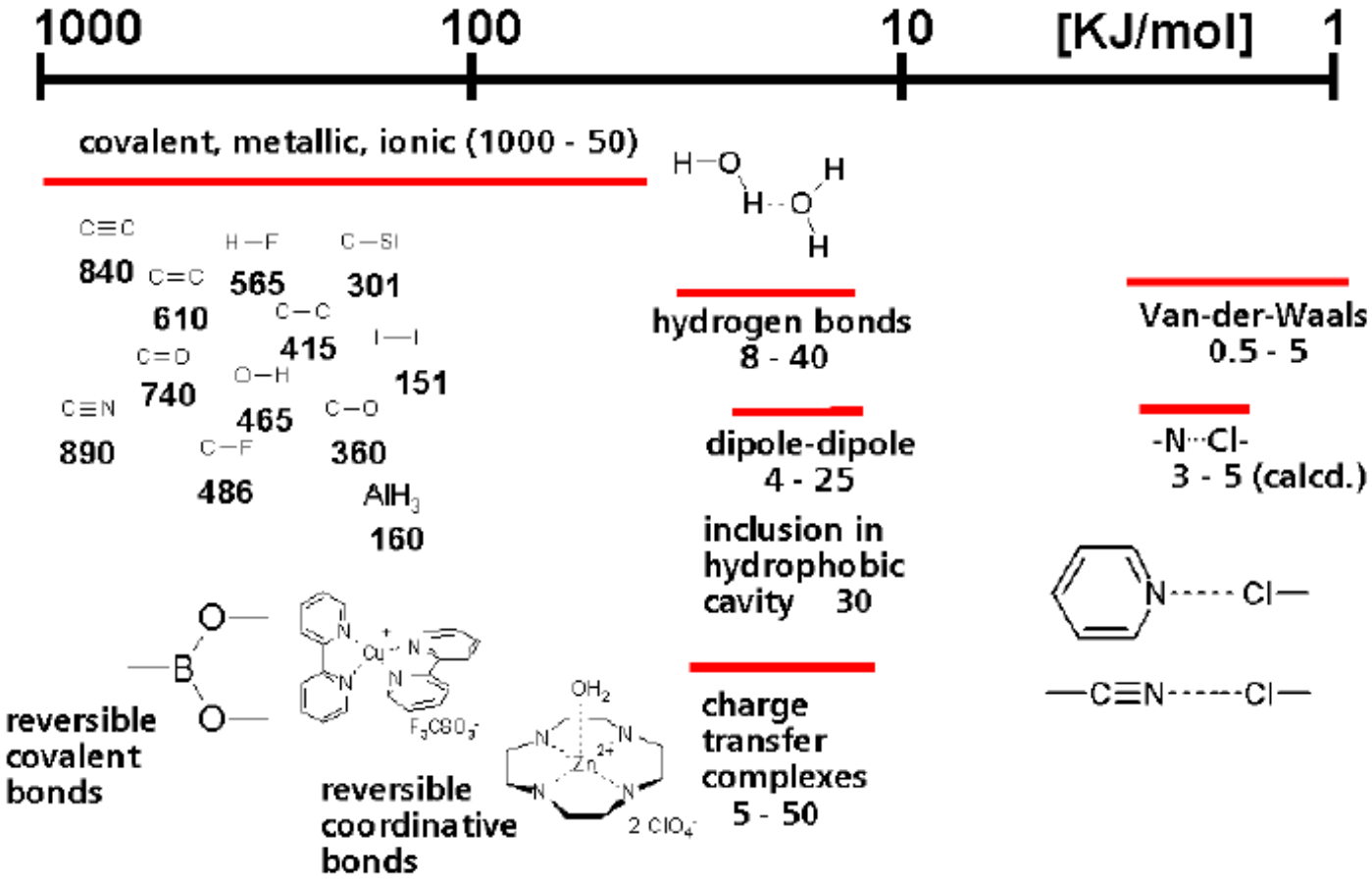

Hydrogen Bonds

A hydrogen bond is the bonding of a covalently attached H-atom with a second atom

Bond energy range: 4 – 120 kJ/mol

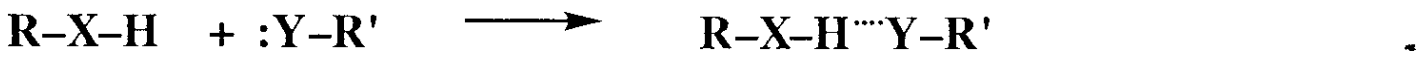

R–X–H : H-bond donor (HO, H_2N, HOOC, H_2NCO, H_2NCOCN_2)

:Y–R' : H-bond acceptor (O-atoms in ROH, ROR', RR'C=O, N-atoms in RR'R''N, N–heterocycles.

Very strong H-bonds are: F–H···F^-, $RCOO^-$···$HN^+(R_2)$–
Strong H-bonds are: O–H···O, O–H···N, N–H···O
moderate H-bonds are: N–H···N
weak H-bonds are: Cl_2C–H···O, Cl_2C–H···N, O–H···π-system of an arene, alkene, or alkyne.

Hydrogen Bonds

Properties of strong, moderate, and weak hydrogen bonds.

	Strong	Moderate	Weak
A—H····B interaction	mostly covalent	mostly electrostatic	electrostatic
Bond lengths	A—H ≈ H····B	A—H < H····B	A—H << H····B
H····B (Å)	~1.2–1.5	~1.5–2.2	2.2–3.2
A····B (Å)	2.2–2.5	2.5–3.2	3.2–4.0
Bond angles (°)	175–180	130–180	90–150
Bond energy (kcal mol^{-1})[a]	14–40	4–15	<4
Relative IR ν_s vibration shift (cm^{-1})[b]	25%	10–25%	<10%
H^1 chemical shift downfield (ppm)	14–22	<14	—
Examples	Gas-phase dimers with strong acids or strong bases Acid salts Proton sponges Pseudohydrates HF complexes	Acids Alcohols Phenols Hydrates All biological molecules	Gas phase dimers with weak acids or weak bases Minor components of 3-center bonds C—H····O/N bonds O/N—H····π bonds

Hydrogen Bonds

Potential energy function along the O···O direction for the water dimer, calculated by *ab initio* MO method at HF/6-31G level. Solid line: Total energy. Broken line: Electrostatic + exchange + mixing energy only.

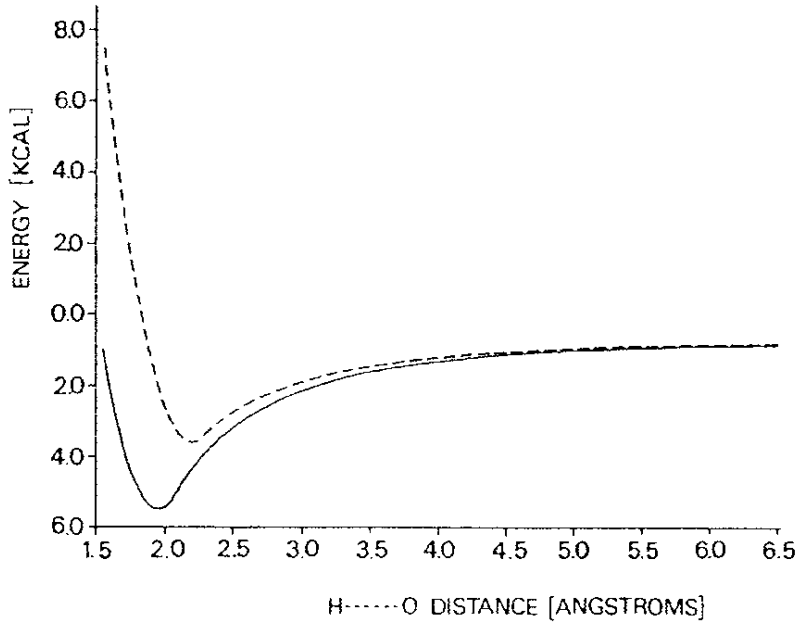

Long Range Interactions: Energy scales with 1/r

Hydrogen Bonds

Structure and Stability of H-Bonds

The force constant for angle bending (angle X–H···Y) is not high and therefore, H-bonds often deviate from linearity (angles often around 160° instead of 180°).

Neutron diffraction studies show frequently bifurcated H-bonds, in which two (H-bond) acceptor atoms are bound to one H-atom (*Figure*).

Neutron diffraction structure of glycine revealing bifurcated H-bonds.

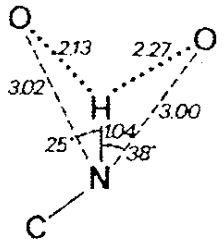

Hydrogen Bonds

DNA Double and Triple Helices

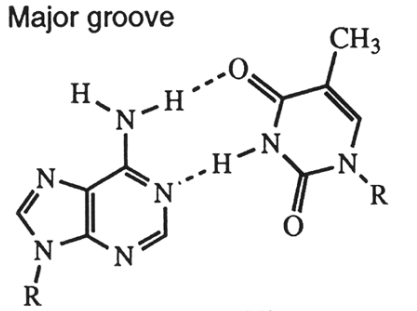

A T

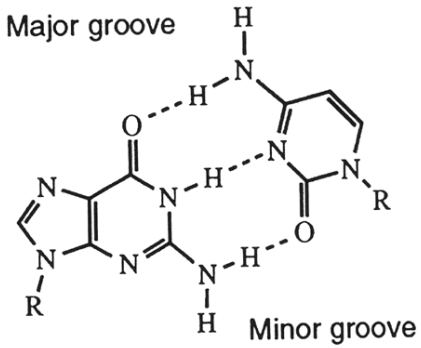

G C

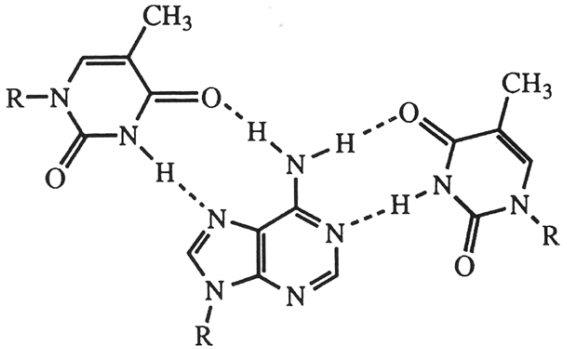

T A T

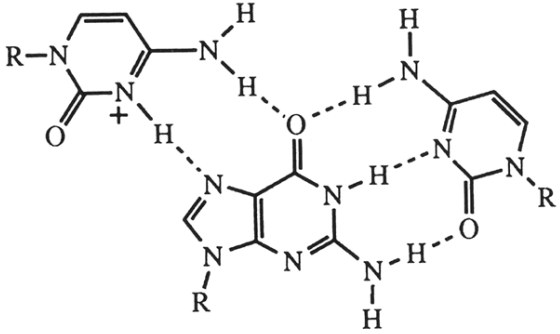

C⁺ G C

Hydrogen Bonds

Secondary Electrostatic Interactions – Important if # of H-Bonds are Identical

1

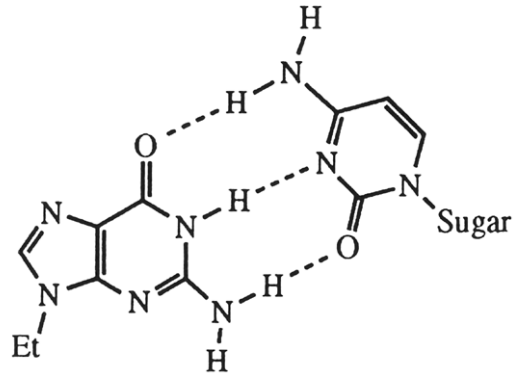

$K_a \approx 10^4 - 10^5$ L mol^{-1}

2

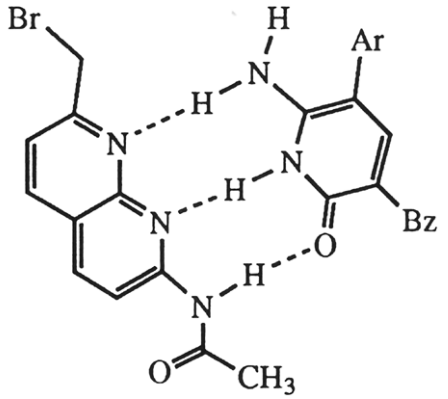

$K_a = 1.7 \times 10^4$ L mol^{-1}

3

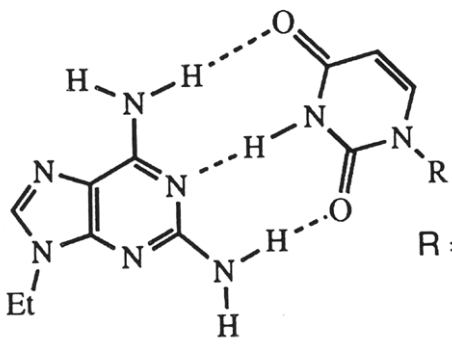

R = cyclohexyl

$K_a \approx 170$ L mol^{-1}

4

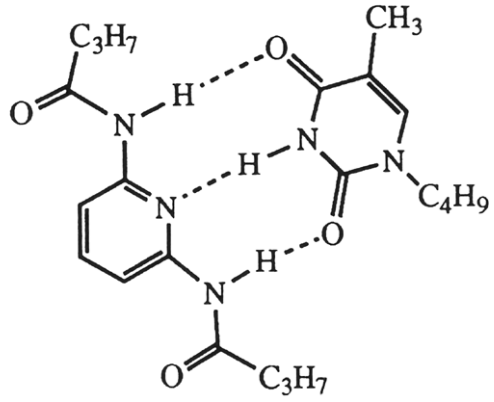

$K_a \approx 90$ L mol^{-1}

Hydrogen Bonds

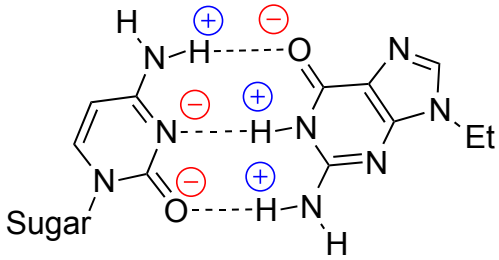

C G

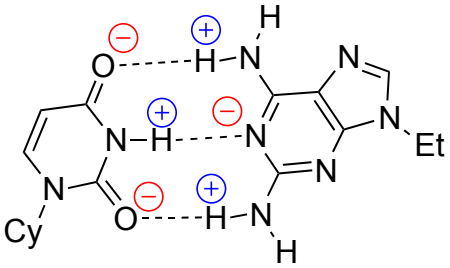

T 2-Aminoadenine

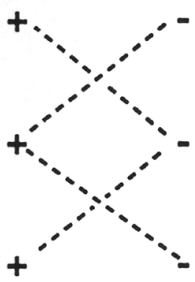

System A:
4 favorable
secondary
interactions

$K_a >> 10^5\ M^{-1}$

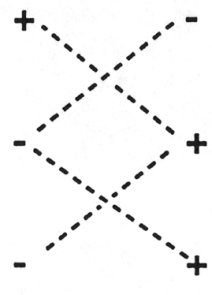

System B:
2 favorable and
2 unfavorable secondary
interactions cancel out

$K_a > 10^4\ M^{-1}$
($CDCl_3$)

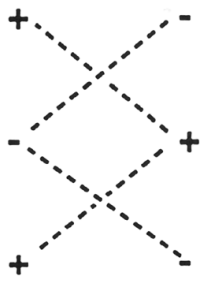

System C:
4 unfavorable
secondary
interactions

$K_a \sim 100\ M^{-1}$

Prior to the model advanced by *Jorgensen*, these differences in stability between base pair associations were not understood.

Hydrogen Bonds

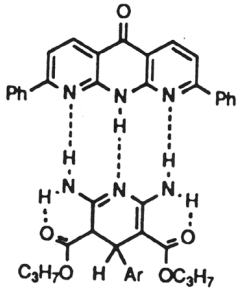

Ar = 2-nitrophenyl

5 (DAD·ADA)
K_a 78 M^{-1}

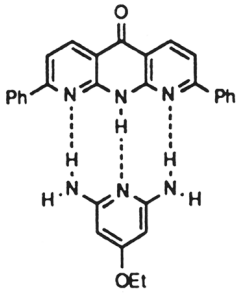

6 (DAD·ADA)
K_a 70 M^{-1} ($CDCl_3$, 298 K)

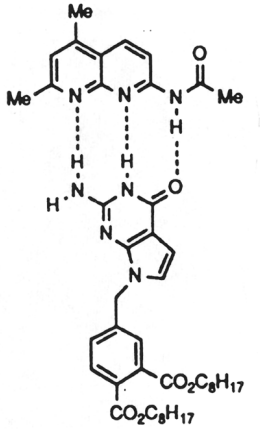

7 (DDA·AAD)
K_a 9.3 x 10^3 M^{-1}

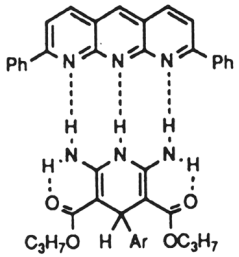

Ar = 3-nitrophenyl

8 (DDD·AAA)
$K_a > 10^5$ M^{-1}

When the model was developed in 1991, a DDD · AAA system was missing. It was later prepared by Zimmerman (*J. Am. Chem. Soc.* 1992, *114*, 4010), confirming the predictions based on consideration of secondary electrostatic effects

Electrostatic Interactions

Ion Paring (Coulombic Interactions)

Coulomb Potential:

$$U_{\text{ion-ion}} = -\frac{1}{4\pi \cdot \varepsilon_o} \cdot \frac{z^+ z^- \cdot e^2}{\varepsilon_r \cdot r}$$

U = potential energy

$z \cdot e$ = ionic charge

ε_r, ε_o = dielectric constant of vacuum (=1) and environment (solvent)

r = distance between ions

Electrostatic Interactions

Ion-pairing often is entropy-driven, due to solvation of the interacting ions

Table. Selected thermodynamic ion-pairing parameters (kcal mol^{-1}) at 298 °C in water.

Ion pair	$\Delta G°$	$\Delta H°$	$T\Delta S°$
$Ca^{2+}\ SO_4^{2-}$	– 3.2	1.6	4.8
$La^{3+}\ Fe(CN)_6^{3-}$	– 5.1	2.0	7.1

- Free enthalpy contribution of **non-buried salt bridges: 1.25 ± 0.25 kcal mol^{-1}**

H. J. Schneider et al. Chem. Soc. Rev. 1994, *23*, 227

Electrostatic Interactions

Ion – Dipole Interactions (50 – 200 kJ/mol)

$$U_{\text{ion-dipole}} = -\frac{1}{4\,\pi\,\varepsilon_o} \cdot \frac{z \cdot e \cdot \mu \cdot \cos\,\theta}{r^2}$$

ε_o = dielectric constant

$z \cdot e$ = ionic charge

r = distance between centers of ion and dipole

μ = dipole moment

θ = angle between dipole and line r.

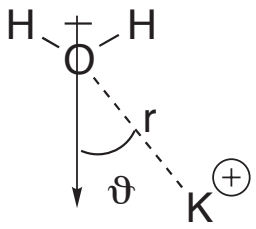

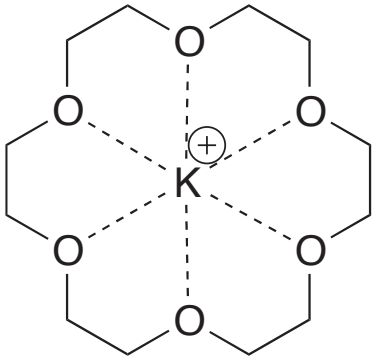

Ion Dipole Interactions at Work

Synthetic Ionophores

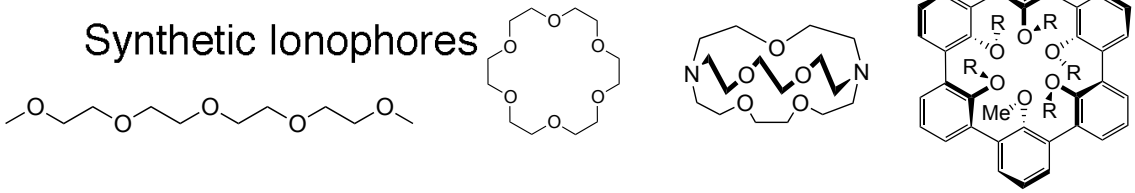

Podands Crown Ether Cryptants Spherands

degree of preorganisation

complex stability constant K_a

$\sim 10^2$ $\sim 10^5$ $\sim 10^8$ $> 10^{10}$

quite similar k_{compl} values, affected mainly by kation desolvation ~ 10^8 - 10^4

complex stabilty is overcome in decomplexation transition state

$10^6\ s^{-1}$ fast on human time scale

$k_{decompl}$

$10^{-12}\ s^{-1}$ slow on human time scale

selectivity

Ion Dipole Interactions at Work – Ion Channels

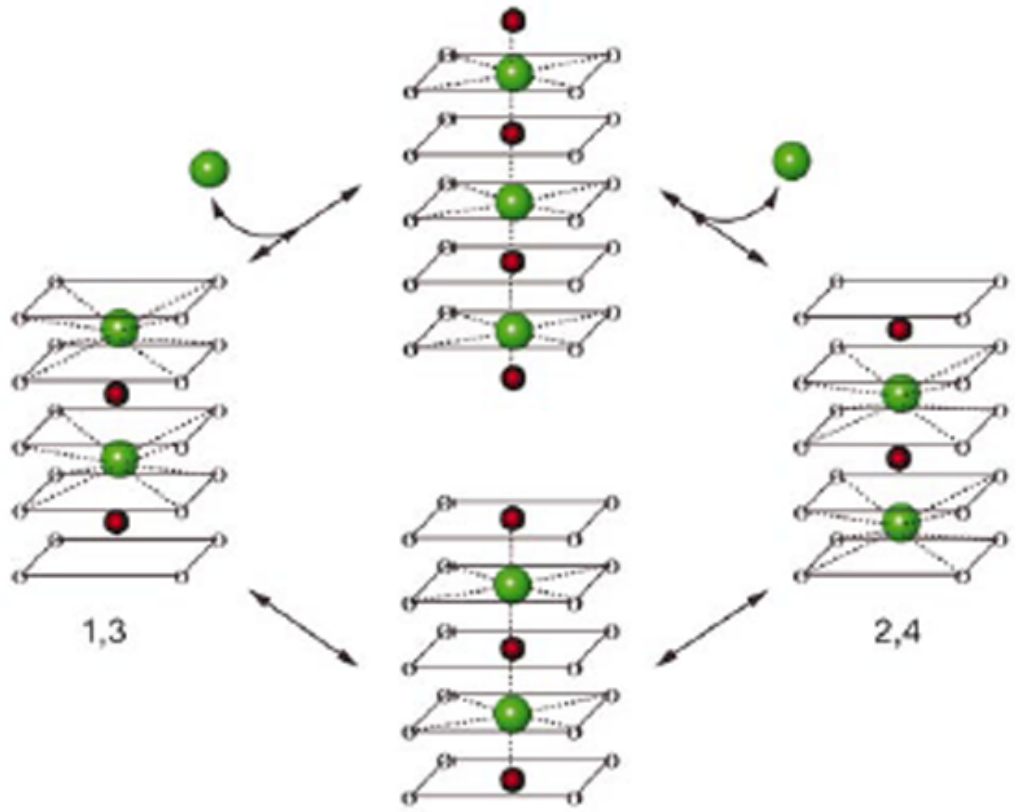

Compare 8-fold coordination by valinomycin and 6-fold Coordination by nonactin

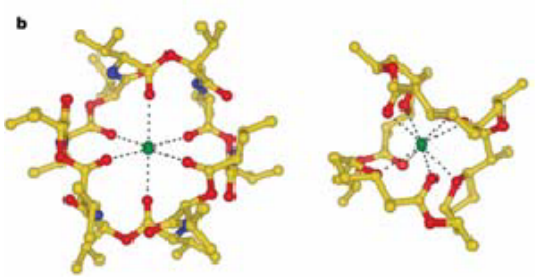

The selectivity filter of the K^+ channel depicted as five sets of four-in-plane O-atoms with K^+ ions (green) undergoing cubic coordination to eight protein C=O groups in the 1,3- and 2,4-configurations. Movement by two paths involves octahedral coordination by six O-atoms, two provided by the intervening H_2O molecules.

Electrostatic Interactions

Dipole – Dipole Interactions (5 – 50 kJ/mol)

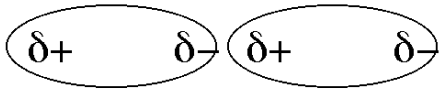

head-to-tail

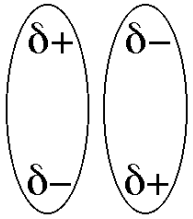

antiparallel

Examples for dipolar interaction

DMSO dimer:

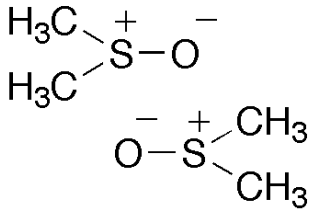

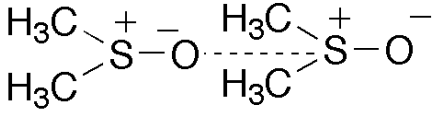

The preferred dipolar alignement is often solvent-dependent: Example: *N*-Methylacetamide:

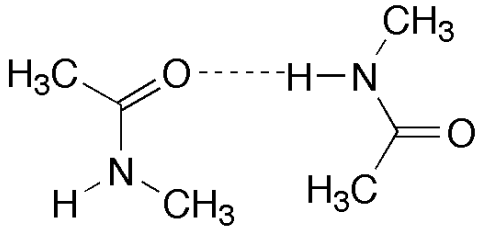

in $CHCl_3$: H-bonding dimer

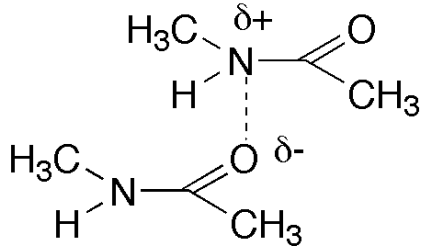

in H_2O: stacking antiparallel dipoles

Electrostatic Interactions

The potential energy of interaction between two polar molecules is a complicated function of the angle between them. However, when the two dipoles are parallel or aligned towards each other, the energy between stationary polar molecules is

$$U_{\text{dipole-dipole}} = \frac{f}{(4\pi\cdot\varepsilon_o)} \cdot \frac{\mu_1 \cdot \mu_2}{r^3}$$

μ = dipole moment
$f = 1 - 3\cos^2\theta$

There is a non-zero average interaction between freely rotating dipoles.

The average potential is

$$U_{\text{dipole-dipole}} = \frac{1}{(4\pi\cdot\varepsilon_o)} \frac{2\,\mu^2_1 \cdot \mu^2_2}{3\,k_B \cdot T \cdot r^6}$$

μ = dipole moment
k_B = *Boltzmann* constant
T = temperature

Dipole-Induced Dipole & Ion-Induced Dipole Interactions

$$U_{\text{dipole-induced dipole}} = -\frac{1}{4\pi\cdot\varepsilon_o}\cdot\frac{2\alpha}{\mu_r^2 6}$$

α = polarizability [Å^3]

Example: H–O–H ··· Cl–Cl; H–O–H···CH_4

$$U_{\text{Ion-induced dipole}} = -\frac{1}{4\pi\cdot\varepsilon_o}\cdot\frac{z^2\cdot e^2\cdot\alpha}{2r^4}$$

Example: I^- ···I–I

Van der Waals or London Dispersion Interactions

London dispersion force (*Van der Waals* Interactions in narrow meaning) + Dipole – Dipole + Dipole – Induced Dipole Interactions

London dispersion force: Instantaneous induced dipole-induced dipole interactions

Lennard-Jones Potential:

$$U = \frac{A}{r^{12}} - \frac{B}{r^{6}}$$

Slater-Kirkwood Equation

$$B = \frac{3/2\ e\ (h/2\pi m^{1/2})\alpha_i\ \alpha_j}{(\alpha_i/N_i)^{1/2} + (\alpha_j/N_j)^{1/2}}$$

e = electron charge

m = electron mass

h = *Planck* constant

N = effective number of electrons in the exterior shell

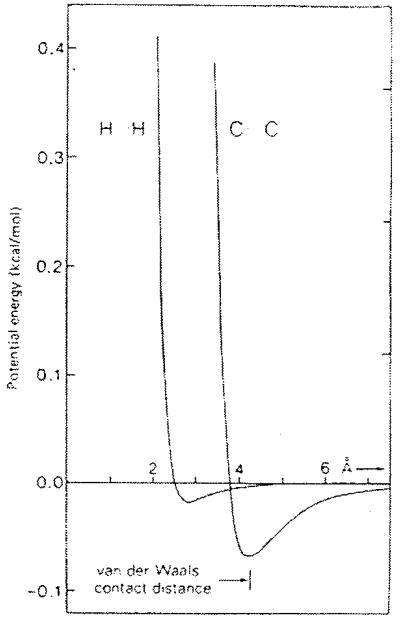

Interaction energies of two H-atoms and two C(sp^3)-atoms in a protein.

Although very weak, dispersion interactions are additive over entire molecule surface and depend on molecular polarizability

Van der Waals or London Dispersion Interactions

Van der Waals forces are responsible for the non-ideal behavior of rare gases and their liquefaction at low temperature. Although weak, they are additive and **represent the major attractive force between apolar solutes.**

=> **Gain in dispersion forces is one of the enthalpic driving forces for apolar complexation in water**

Aromatic Aromatic Interactions

a)

T-shaped,
edge-to-face

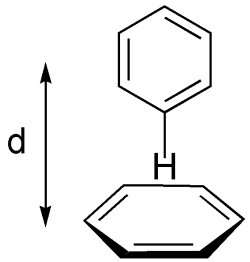

6

b)

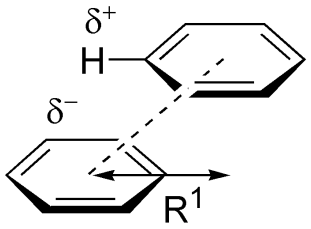

parallel displaced
π-π stacking

7

c)

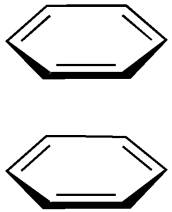

eclipsed
π-π stacking (the least favorable one)

8

Geometry: Ring-center separation in **6**: 4.96 Å

Interplanar distance in **7**: 3.4 - 3.6 Å with a displacement R^1 of 1.6 - 1.8 Å.

Energetics: T-shaped geometry in gas phase: –6.7 ± 0.9 kJ/mol; T-shaped preferred in water by –6.1 kcal/mol

Aromatic Aromatic Interactions in Proteins

• *Burley and Petsko*: 60% of aromatic side chains (Phe, Trp, Tyr) are involved in *π-π* interactions with the **T-shaped edge-to-face structure being predominant** (*Adv. Protein Chem.* 1988, *39*, 125)

• *McGaughley et al:* A larger protein sampling finds the **parallel-displaced** geometry as the preferred one (*J. Biol. Chem.* 1998, *273*, 15458)

None of the studies describes the face-to-face eclipsed stacking geometry!

•**Interaction free enthalpy increments for the Phe···Phe pair** in the self-association of a 12-residue beta-hairpin or in the cold-shock protein CspA were estimated as ≈ **- 2.3 kJmol^{-1}**
(*C. D. Tatko, M. L. Waters*, *J. Am. Chem. Soc. 2002*, *124*, 9372; B. J. Hillier et al. *Folding Des.* 1998*, 3,* 87)

Stabilization of alpha-helices by **Phe···Phe** interactions: **–3.3 kJ mol^{-1}**
(*M. L. Waters et al., J. Am. Chem. Soc.* 2002, *124*, 9751)

Aromatic Aromatic Interactions in Proteins

London dispersion interactions are the **major stabilization** energy between two aromatics

However, the **electrostatic component associated with the large quadrupole moment of benzene** is an influential factor determining the **geometry** of interaction

In **aqueous solution, hydrophobic effects** need to be additionally considered. The calculated Gibbs free energy minimum for the benzene dimer is

in liquid benzene:	–1.7 kJ/mol
in chloroform:	–4.2 kJ/mol
in water:	–6.3 kcal/mol

Also **in water, the T-shaped structure is the most stable one.**

(*W. L. Jorgensen, D. L. Severance*, *J. Am. Chem. Soc.* 1992, *114*, 4366, *Kollman et al., J. Am. Chem. Soc.* 1996, *118*, 11217)

Toluene dimers actually might be better models for biological *π*-*π* interactions; due to the small dipole originating from the Me-group, a **stacked** arrangement is the global minimum (*Gervasio et al., J. Am. Chem. Soc.* 2002, *106*, 2945)

Hydrogen Bonding to Aromatic Systems

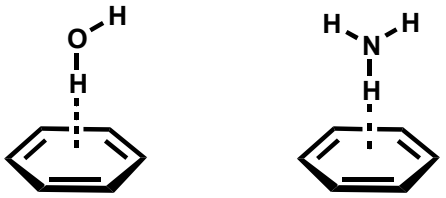

E_{total} / kcal mol^{-1} –3.02 –2.22

CCSD(T); S. Tsuzuki, *Struct. Bond.* **2005**, *115*, 149–193.

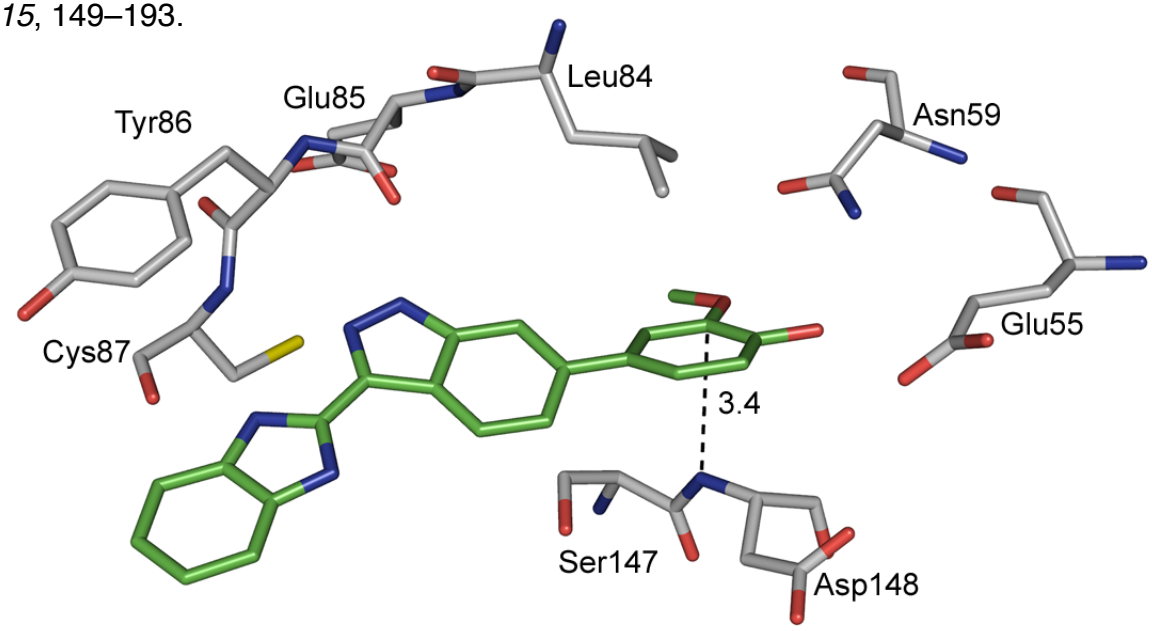

Resolution: 2.60; PDB code: 2C3K; N. Foloppe, L. M. Fisher, G. Francis, R. Howes, P. Kierstan, A. Potter, *Bioorg. Med. Chem.* **2006**, *14*, 1792–1804.

Cation-Π Interactions

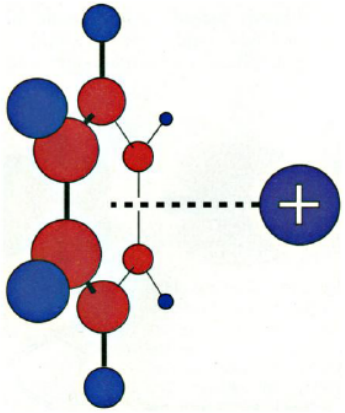

Strength in biol systems **-1.7 - -10 kJ/mol** (Lys, His, Arg - Trp, Tyr, Phe) i.e. ca. **Factor of 10** in Binding

Experimental gas-phase measurements

cation	binding energy Δ*H* to benzene	
Li^+	38.3	160
Na^+	28.0	117
K^+	19.2	80
NH_4^+	19.3	80
NMe_4^+	9.4	39

e.g. Li^+, Na^+, K^+

protonated amines

quaternary ammoniums

sulfoniums

K^+···water 75 kJ mol^{-1} in the gas phase

J. Sunner, K. Nishizawa, P. Kebarle, *J. Phys. Chem.* **1981**, *85*, 1814–1820.

In optimal geometry cation over the centre of the ring, along the 6-fold axis

J. C. Ma, D. A. Dougherty, *Chem. Rev.* **1997**, *97*, 1303–1324.

Cation-Π Interactions

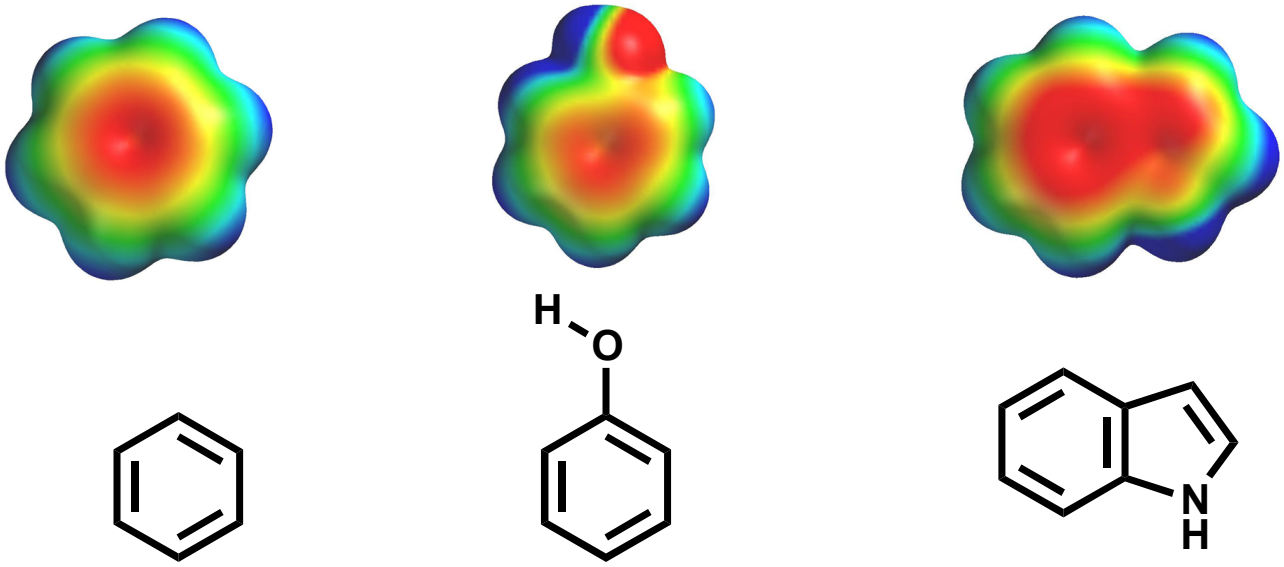

Spartan, HF/3-21*, scale –27 to +21.

PDB:

- On average one cation–π interaction for every 77 amino acid residues in a protein
- 26% of Trp, preference for the 6-membered ring
- Trp > Tyr >> Phe; His not found!
- Arg >> Lys
- Lys interacts through ε-carbon rather than ammonium moiety

S. Mecozzi, A. P. West, Jr., D. A. Dougherty, *Proc. Natl. Acad. Sci.* **1996**, *93*, 10566–10571; D. A. Dougherty, *Science* **1996**, *271*, 163–168; J. P. Gallivan, D. A. Dougherty, *Proc. Natl. Acad. Sci.* **1999**, *96*, 9459–9464.

Cation-Π Interactions

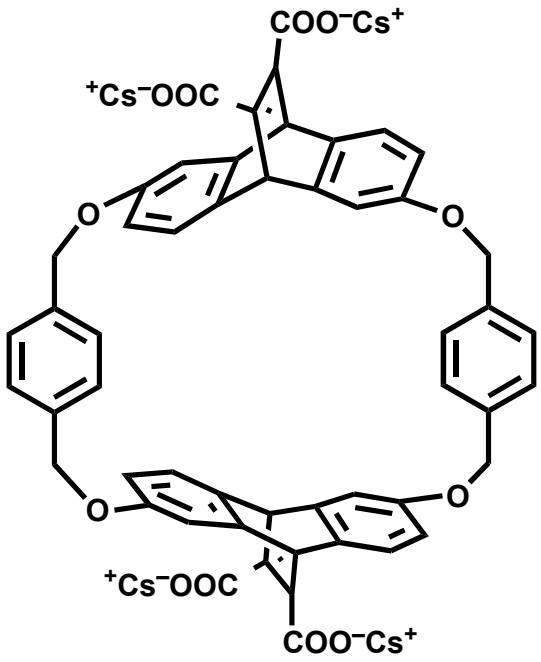

	ΔG (kcal mol^{-1}) in buffer pD = 9
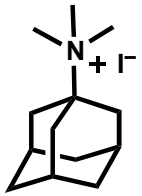	6.7
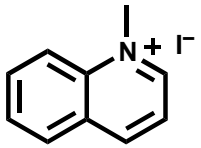	7.6
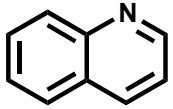	5.4
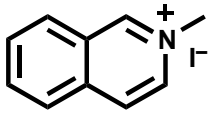	7.2
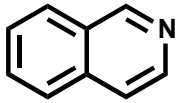	6.3

T. J. Shepodd, M. A. Petti, D. A. Dougherty, *J. Am. Chem. Soc.* **1986**, *108*, 6085–6087.
M. A. Petti, T. J. Shepodd, R. E. Barrans, Jr., D. A. Dougherty, *J. Am. Chem. Soc.* **1988**, *110*, 6825–6840.
T. J. Shepodd, M. A. Petti, D. A. Dougherty, *J. Am. Chem. Soc.* **1988**, *110*, 1983–1985.

Cation-Π Interactions in Factor Xa Inhibition

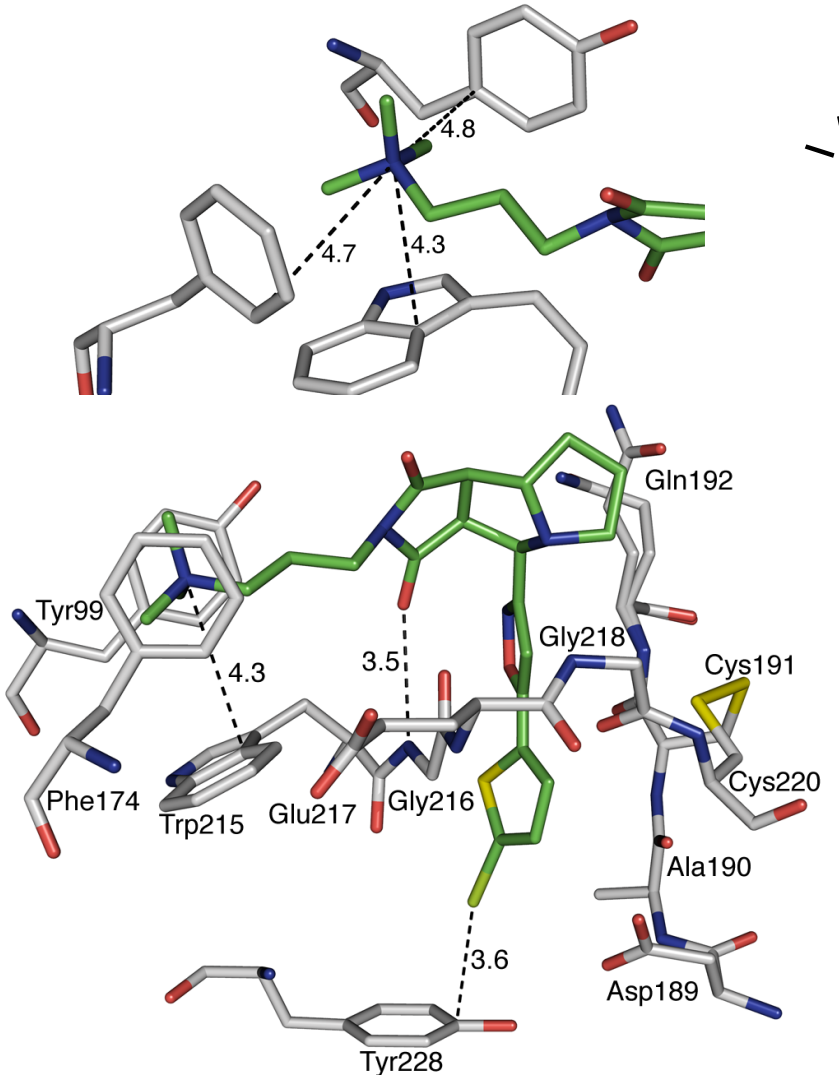

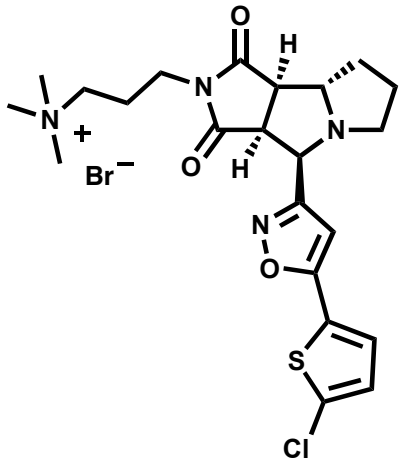

(±)-**34**

K_i(FXa) = 9 nM

K_i(Thr) > 35.1 μM

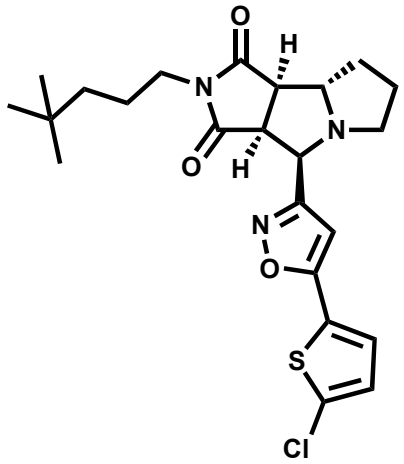

(±)-**81**

K_i(FXa) = 550 nM

K_i(Thr) = 17.8 μM

ΔΔ*G* = 10 kJ/mol

Solved by Dr. D. W. Banner at F. Hoffmann-La Roche, resolution 1.25 Å, PDB code: 2JKH.

L. M. Salonen, C. Bucher, D. W. Banner, W. Haap, J.-L. Mary, J. Benz, O. Kuster, P. Seiler, W. B. Schweizer, F. Diederich, *Angew. Chem. Int. Ed.* **2009**, *48*, 811–814.

Cation-Π Interactions in Factor Xa Inhibition

R	K_i / nM
H_2N	9800
N H	911
N	56
N + Br −	9

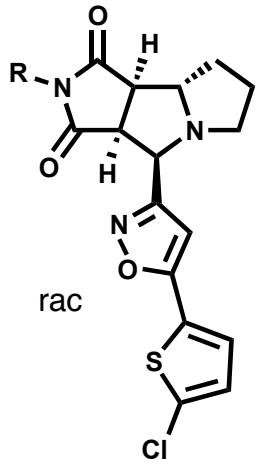

R	K_i / nM
	10300
	1400
	750
	550

Factor of 10 in Binding for Each Methyl Group ...

L. M. Salonen, M. C. Holland, P. S. J. Kaib, W. Haap, J. Benz, J.-L. Mary, O. Kuster, W. B. Schweizer, D. W. Banner, F. Diederich, *Chem. Eur. J*, in press.

Anion Binding

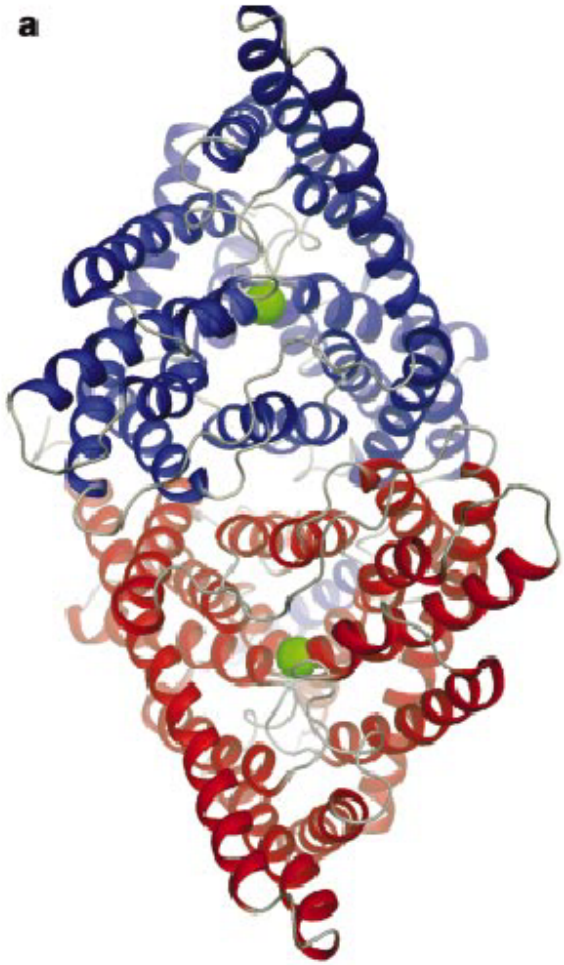

View from the extracellular side of the CIC chloride channel that catalyzes selectively the flow of Cl^- across cell membranes, thereby regulating electrical excitation in skeletal muscle and the flow of salt and water across epithelial barriers.

The channel is a **homodimer membrane protein** in which a Cl^- ion is stabilized by **electrostatic interactions with α-helix dipoles and by interactions with N–H and O–H groups**

Anion Binding

Ca. 70% of all biological substrates are anions, which adds interest to studies of anion recognition by artificial receptors.

However, due to their **very large solvation free energies**, anions are difficult to complex. **It usually requires ion pairing and ionic H-bonds, *i.e. Coulombic* attraction.**

X-ray, C_9-bridges

N^+-H •••• Cl^- ••• H-N^+
< 3.10 Å >

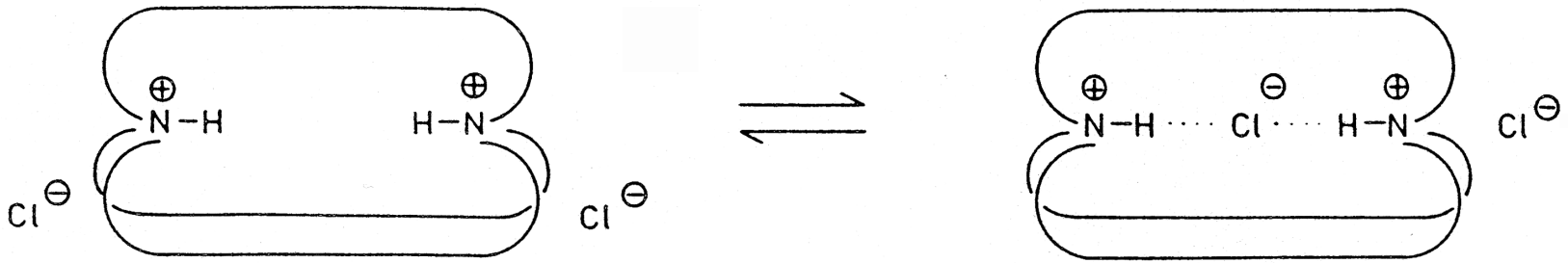

Simmons and *Park, Dupont 1968*: the endo-endo-protonated cryptand binds Cl^- by two ionic H-bonds.
=> both first cation and anion receptors synthesized at Dupont.

Potent Anion Binders

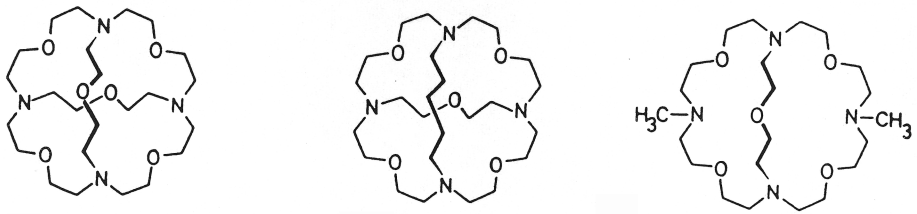

(Lehn)

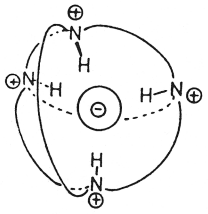

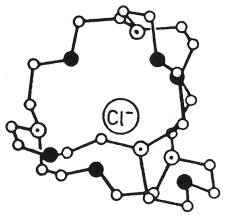

crystal structure

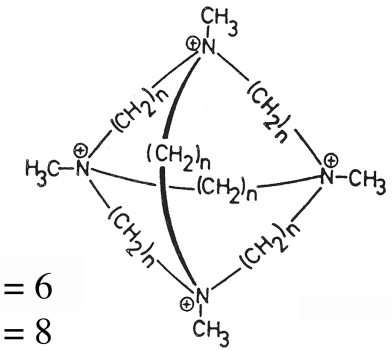

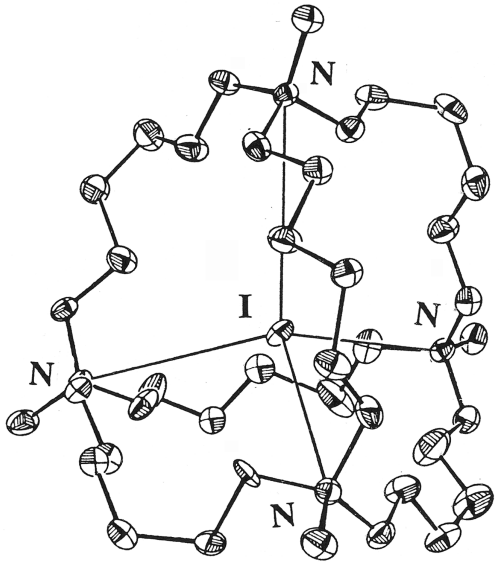

Host **1** in H_2O:

log K_a (Br^-) = 1.5

log K_a (Cl^-) > 4.5

$\Rightarrow \Delta(\Delta G)$ = 4 kcal mol^{-1}

(high due to preorganization)

(*Schmidtchen*)

Potent Anion Binders

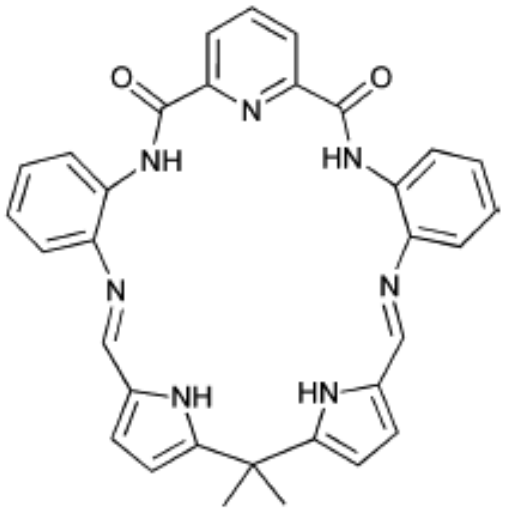

1

Table 1 Affinity constants for the binding of anions by receptor **1** as determined from UV-vis spectroscopic titrations in CH_3CN. The anions studied were in the form of their tetrabutylammonium salts

Anion	K_a (mol dm^{-3})[a]
Br^-	[b]
NO_3^-	[b]
Cl^-	2000 ± 23
CN^-	12,000 ± 2500
CH_3COO^-	38,000 ± 3000
HSO_4^-	64,000 ± 2600
$H_2PO_4^-$	342,000; 26,000[c]

Proposed HSO_4^- complex geometry

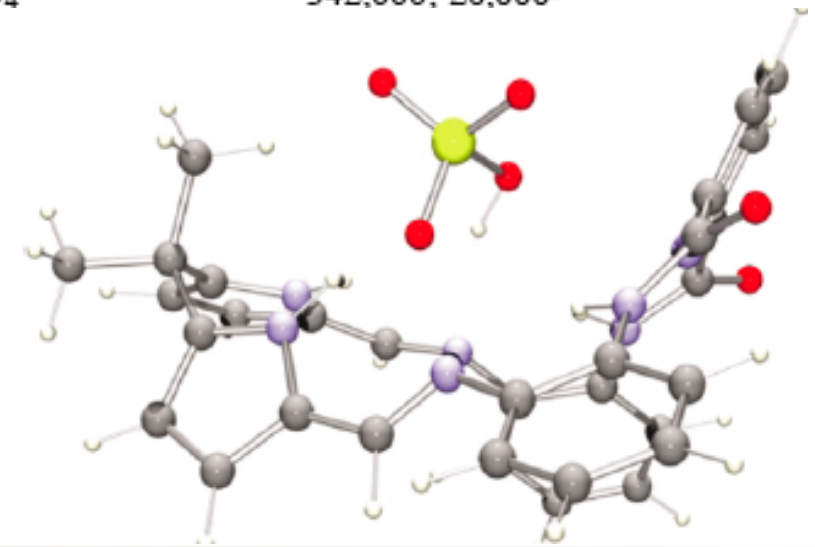

J. Sessler et al. Chem. Commun. 2004, 1276

Phosphate Binding in Biology

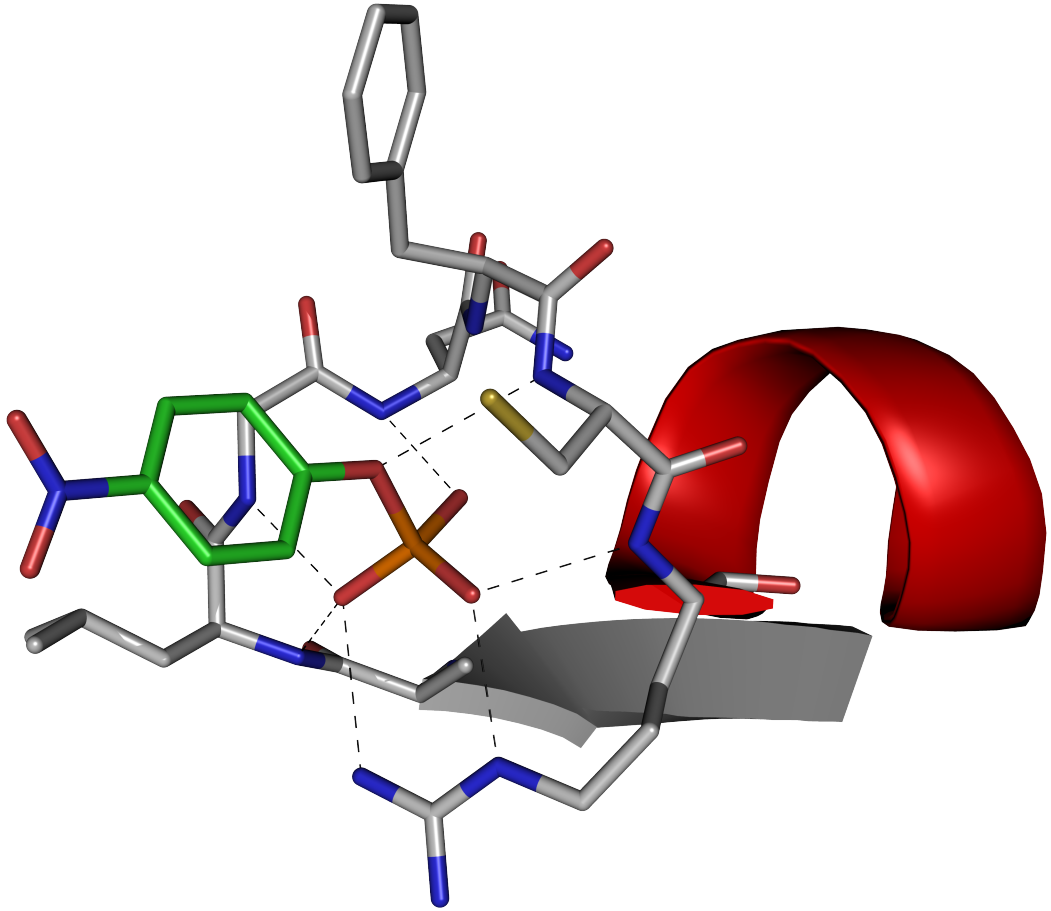

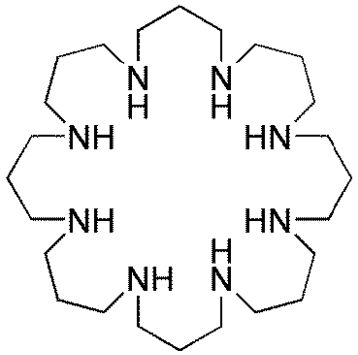

A protein tyrosine phosphatase (1D1Q) in complex with *p*-nitrophenol

A. Hirsch, F. Fischer, F. Diederich, *Angew. Chem.* **2007**, *46*, 338-352

Phosphate Binding in Biology

• analogies to synthetic anion receptors:

- phosphate anions organize the receptor site
- loop wraps around the anion
- H-bonds with converging backbone amide N-H

• statistical analysis:

- highly characteristic distribution of aa in various classes of enzymes
- **82%** show phosphate binding ***without a metal***
- **36%** show phosphate binding ***with neither a metal nor Arg/Lys***

• outlook:

- 36% feature “neutral” bindig sites which can be filled by small ***heteroalicyclic*** or ***heteroaromatic*** residues having extended H-bond acceptor functionalities

A. Hirsch, F. Fischer, F. Diederich, *Angew. Chem.* **2007**, *46*, 338-352

Halogen Binding

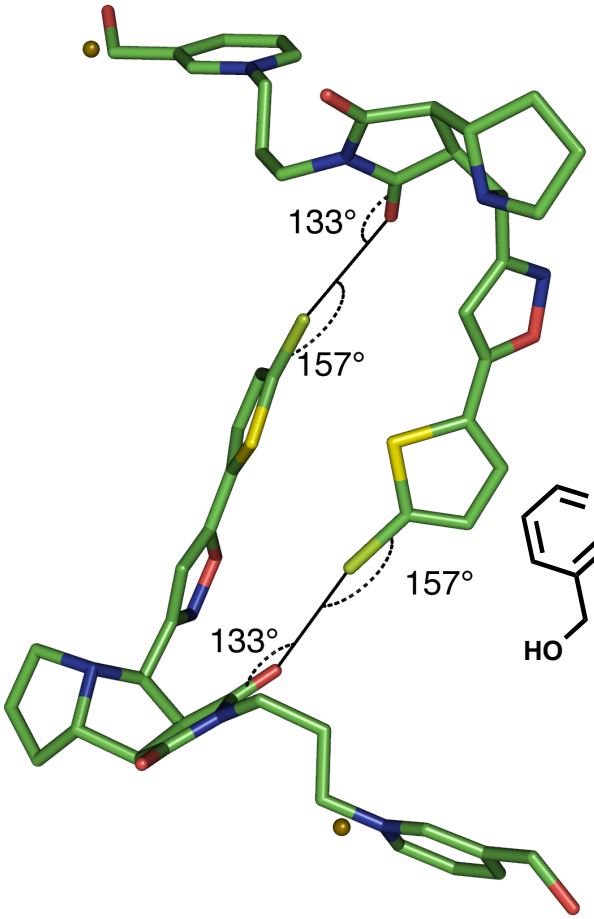

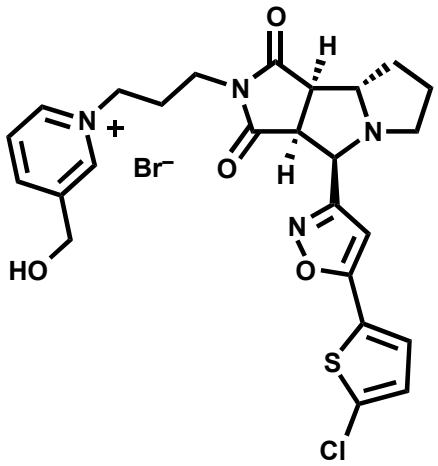

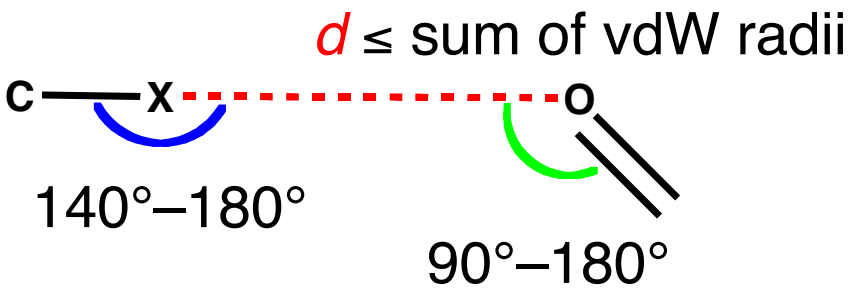

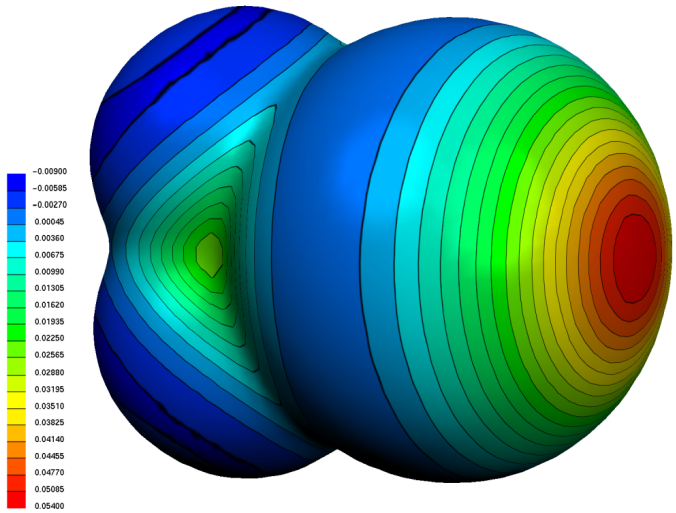

T. Clark, M. Hennemann, J. S. Murray, P. Politzer, *J. Mol. Model.* **2007**, *13*, 291–296.
O. Hassel, J. Hvoslef, *Acta Chem. Scand.* **1954**, *8*, 873.
Reviews: P. Metrangolo, F. Meyer, T. Pilati, G. Resnati, G. Terraneo, *Angew. Chem. Int. Ed.* **2008**, *47*, 6114–6127; E. Parisini, P. Metrangolo, T. Pilati, G. Resnati, G. Terraneo, *Chem. Soc. Rev.* **2011**, *40*, 2267–2278.

Literature

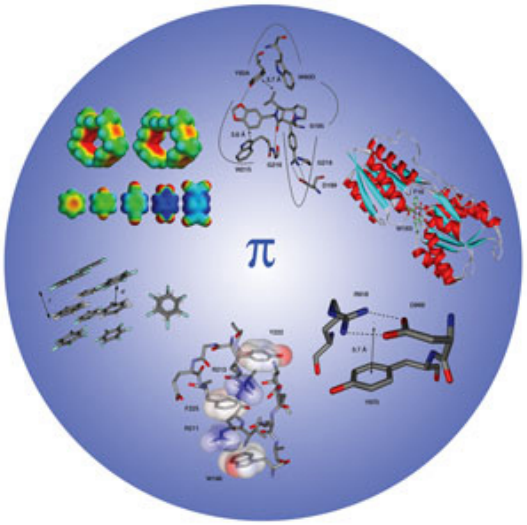

Interactions with Aromatic Rings in Chemical and Biological Recognition E. A. Meyer, R. K. Castellano, F. Diederich *Angew. Chem. Int. Ed.* **2003**, *42*, 1210-1250.

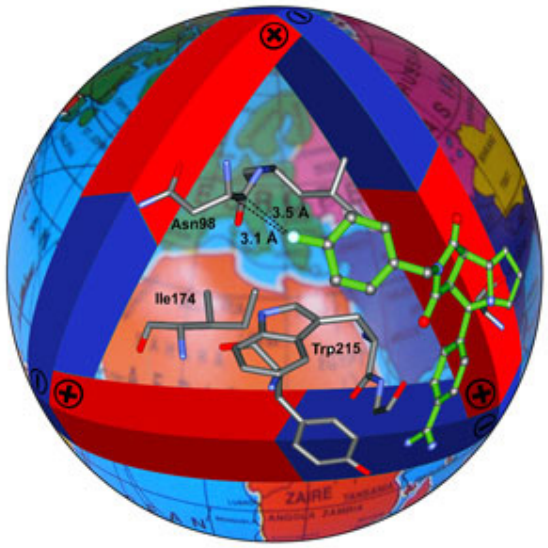

Orthogonal Multipolar Interactions in Structural Chemistry and Biology R. Paulini, K. Müller, F. Diederich *Angew. Chem. Int. Ed.* **2005**, *44*, 1788-1805

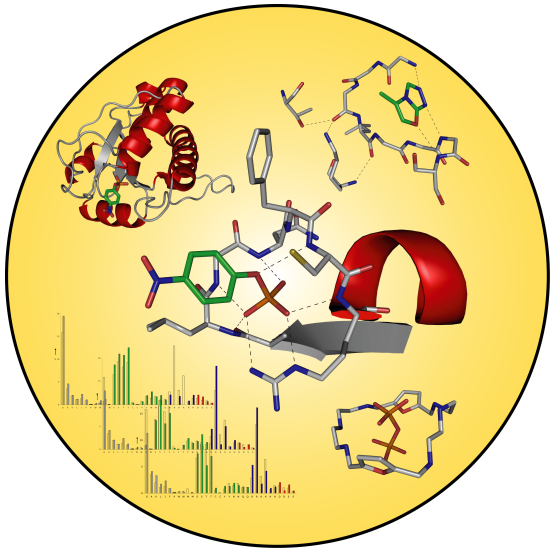

Phosphate Recognition in Structural Chemistry and Biology A. Hirsch, F. Fischer, F. Diederich, *Angew. Chem. Int. Ed.* **2007**, *46*, 338-352

Classical Hydrophobic Effect

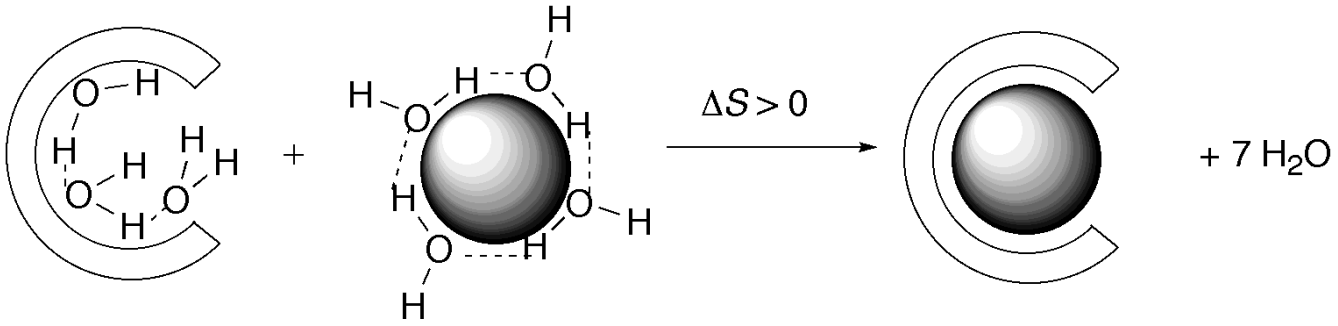

Thermodynamic quantities characteristic for binding driven by the classical hydrophobic effect, are:

1. **a large favorable complexation entropy $T\Delta S^{o}$**,
2. a small complexation enthalpy ΔH^{o}, and
3. a large negative change in heat capacity $\Delta C_p{}^{o}$.

The classical hydrophobic effect had originally been defined to account for the thermodynamic characteristics measured for the transfer of small apolar solutes from the gas phase into water.

These quantities are measured for **loose associations (membranes, micelles) and for large surface desolvation (protein folding)** (*N. T. Southall, K. N. Dill, A. D. J. Haymet*, *J. Phys. Chem. B.* 2002, *106*, 521)

Hydrophobic Effect

Origin of the Definition of the Classical Hydrophobic Effect:
Transfer of Small Solutes into Water

$$\Delta G = \Delta H - T\Delta S$$

Table. Thermodynamic parameters (kJ mol^{-1}) of transfer of some hydrocarbon solutes from gas phase and from organic solvents to water at 298 K (standard state 1 atm gas and unit mole fraction solution).

Solute	*Transfer from*	ΔG	ΔH	$T\Delta S$	ΔC_p[a]
CH_4	gas	26.28	-13.81	-40.09	217
	n-hexane	13.14	-11.55	-25.69	
	methanol	8.79	-5.86	-14.65	
C_3H_8	gas	26.07	-22.51	-48.58	319
	n-hexane	20.63	-8.41	-29.04	
	methanol	14.94	-6.15	-21.09	
n-C_6H_{14}	gas	28.53	-31.38	-59.91	440
	n-hexane	32.55	0.17	-32.38	
	methanol	24.35	-0.46	-24.81	

[a] in J mol $^{-1}$ K $^{-1}$.

Hydrophobic Effect

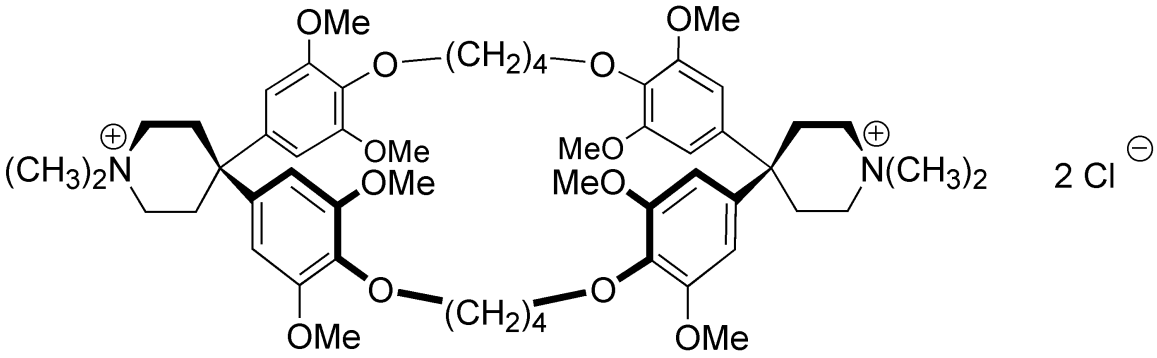

1

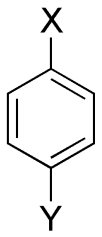

	X	Y
2a	COOMe	COOMe
2b	Me	NO_2
2c	HO	NO_2
2d	MeO	MeO
2e	Me	Me

Water-soluble Cyclophanes Mimic the Aromatic Binding Pockets at Enzyme Active Sites

Nonclassical Hydrophobic Effect

Enthalpic Driving Force for the Complexation of Benzene Derivatives by the Spherical Hemicarcerand Host 3 (in aq. borate buffer pH 9)

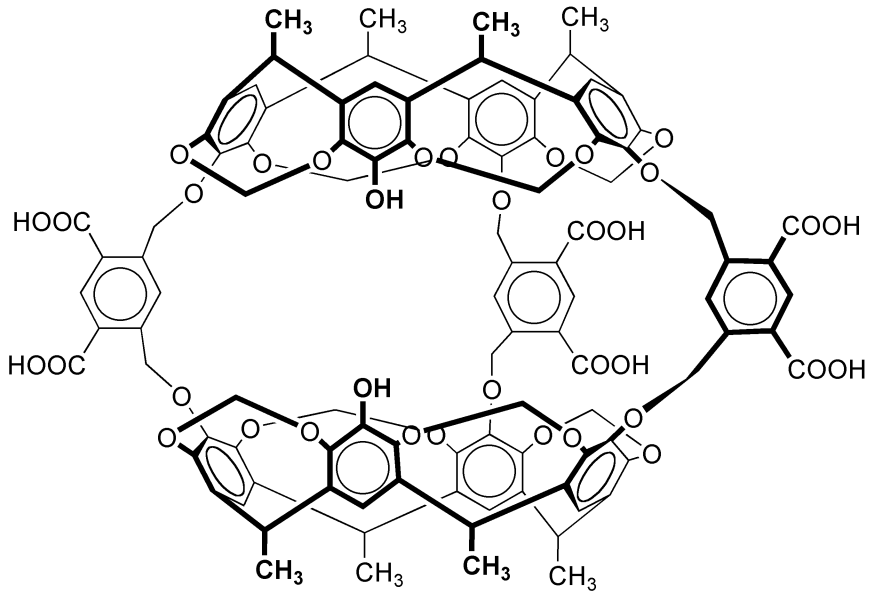

3

K. Deshayes et al. Chem. Eur. **2000**, *6*, 999

Guest	$\Delta G^{o}_{293\ K}$ [kcal mol^{-1}]	$\Delta H^{o}_{293\ K}$ [kcal mol^{-1}]	$T\Delta S^{o}_{293\ K}$ [kcal mol^{-1}]
2d	−7.9	−10.9	−3.0
2e	−9.6	−12.3	−2.6

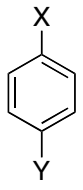

	X	Y
2a	COOMe	COOMe
2b	Me	NO_2
2c	HO	NO_2
2d	MeO	MeO
2e	Me	Me

Nonclassical Hydrophobic Effect

In addition to the entropically driven association, many complexation processes in water are **enthalpically driven**.

$$\Delta G = \Delta H - T\Delta S$$

The **enthalpic solvophobic driving force** has two components:

(i) **Gain in dispersion interactions.** Upon complexation, weak **van der Waals interactions** between poorly polarizable H_2O molecules and hydrocarbon surfaces are replaced by stronger contacts between CH, CH_2, and CH_3 groups of the binding partners. The exchange of weaker $CH_x\cdots O$ by stronger $CH_x\cdots CH_x$ interactions provides a favorable gain in enthalpy.

See: E. Meyer, R. C. Castellano, F. Diederich, Angew. Chem. Int. Ed. **2003**, *42*, 1210-1250

Nonclassical Hydrophobic Effect

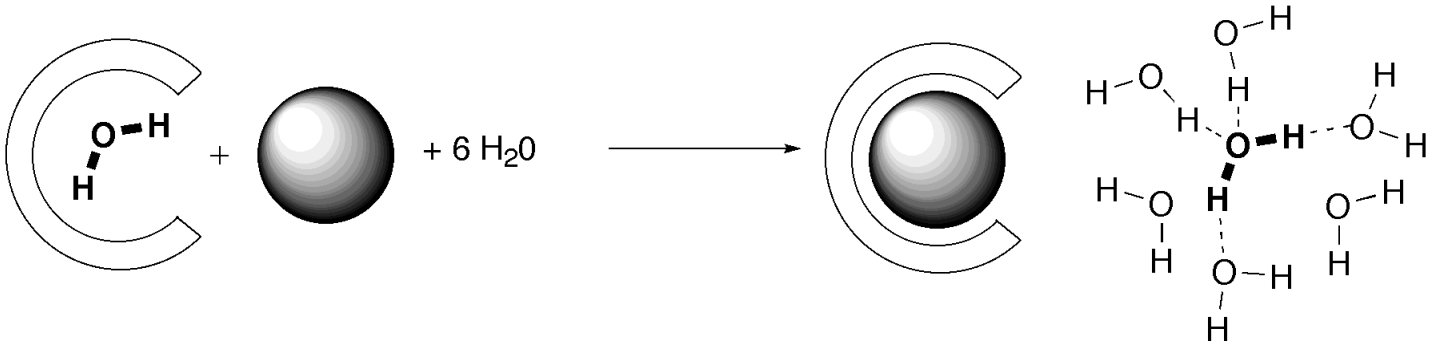

(ii) Water molecules around apolar surfaces and in apolar binding sites are unable to form four H-bonds. When these surface water molecules are transferred into the bulk upon complexation, full H-bonding interactions are re-gained, thereby leading to a **gain in solvent cohesive interactions**. Water has the highest cohesive energy of all solvents and, therefore, the **cohesive enthalpic** gain is highest in this solvent.

* Other formulation of this point: **Water in deep apolar binding pockets has a high unfavorable enthalpy** ("strained water").

* Or: If water molecules are removed from the H-bonding settings in the bulk in order to solvate apolar surfaces, a cavity is formed in the solvent. This cavitation is **enthalpically** unfavorable and, upon transferring these H_2O-molecules back into the bulk, the energy initially required for **cavitation**, is regained (*Sinanoglu* (Yale)).

Nonclassical Hydrophobic Effect

A **summary** of many biological and chemical binding studies reveals that

→ **Loose association** (as in the formation of micelles and membranes or in complexes where the contacts between the binding partners are not very tight) as well as association processes **involving large surfaces** (protein folding) are most often **entropically** driven.

→ **Tight association** of small guests (in narrow binding pockets) is **enthalpically** controlled.

Complexation in water of large apolar guests such as steroids may well be both enthalpically and entropically favorable.

Nonclassical Hydrophobic Effect

Strong enthalpic driving force ($\Delta H << 0$) for complexation, partially compensated by an unfavorable entropic term ($T\Delta S < 0$)

measured in aqueous solution for:

- cyclophane-arene inclusion complexation

- cyclodextrin complexation

- enzyme-substrate binding

- antibody recognition

- DNA intercalation by arenes such as ethidium bromide

- DNA association with intercalator/minor groove binders such as the antitumor drug daunomycin

- DNA minor groove intercalation of antitumor drugs such as netropsin and distamycin as well as hairpin polyamides

- protein-protein,protein-DNA, and protein-lipid interactions.

E. A. Meyer, R. K. Castellano, F. Diederich, Angew. Chem. Int. Ed. 2003

Thermodynamic Quantities Reflect Tightness of Fit

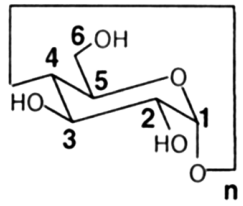

n = 6 α– CD

n = 7 β– CD

n = 8 γ– CD

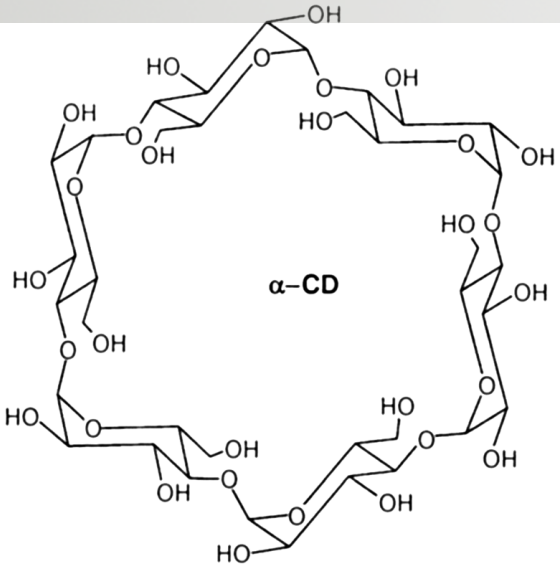

Cyclodextrins

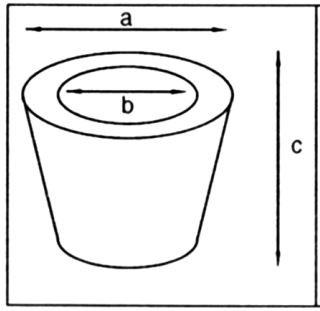

CD	a	b	c
α-CD	13.7	4.5	6.7
β-CD	15.3	7.0	7.0
γ-CD	16.9	9.5	7.8

Scheme B 20. α-,β-,γ-Cyclodextrins with cavity dimensions (Å).

W. C. Cromwell, K. Bystrom, M. R. Eftink, *J. Phys. Chem.* **1985**, *89*, 326-332.

guest:	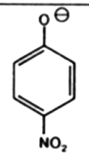	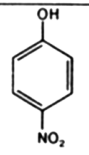	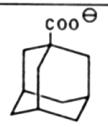
α-CD			
-ΔG	18.7	11.5	11.6
-ΔH	42.8	23.0	14.3
TΔS	-24.1	-11.5	-2.7
β-CD			
-ΔG	15.0	14.2	24.5
-ΔH	16.1	10.2	21.6
TΔS	-1.1	3.9	2.9

Scheme B 21. Thermodynamic data [kJ mol^{-1}] for selected cyclodextrin complexes.

1:1 Binding of adamantanecarboxylate in γ:

$-\Delta G$ = 20.2 kJ/mol

$-\Delta H$ = –5.3 kJ/mol

$T\Delta S$ = 26.4 kJ/mol

Enthalpy-Entropy Compensation

A Nearly Universal Finding in Molecular Recognition in Chemistry and Biology

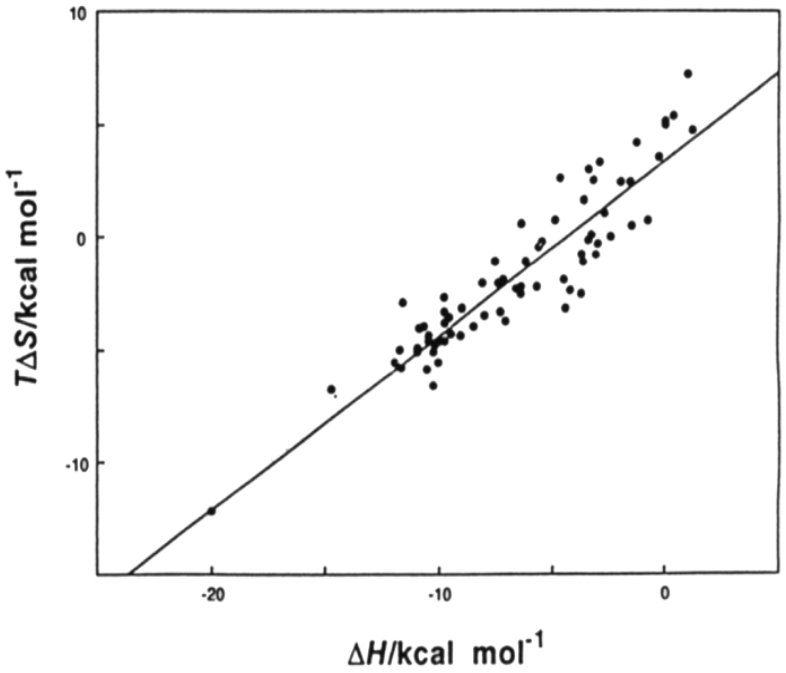

Benzene derivatives + cyclophanes and calixarenes.

Y. Inoue et al. J. Am. Chem. Soc. 1993, *115*, 10637

J. D. Dunitz, Chem. Biol. 1995, *2*, 709

L. Liu, Q.-X. Guo, Chem. Rev. 2001, *101*, 673

For recent work on enthalpy/entropy compensation in biology, see: V. M. Krishnamurthy, B. R. Bohall, V. Semetey, G. M. Whitesides, *J. Am. Chem. Soc.* **2006**, *128*, 5802-5812

Enthalpy-Entropy Compensation

Preorganization Maybe Accompanied by Entropic Penalties in Protein-Ligand Interactions

Table 1: Thermodynamic parameters for complex formation between the Grb2 SH2 domain and pseudopeptides **2–7**.[a]

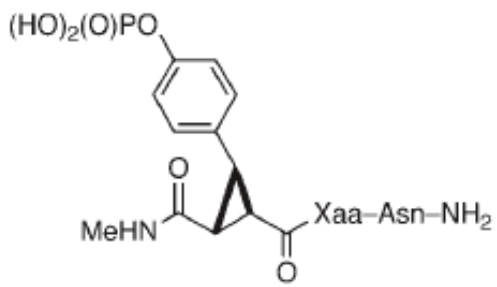

2: Xaa = Val
4: Xaa = Ile
6: Xaa = Leu

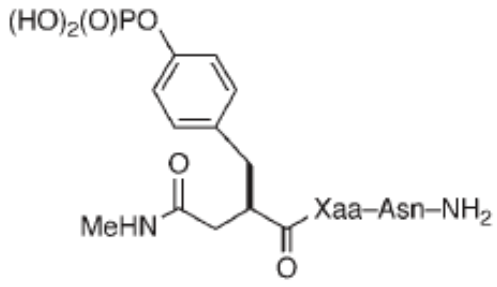

3: Xaa = Val
5: Xaa = Ile
7: Xaa = Leu

Cmpd.	K_a [M^{-1}]	ΔG [kcal mol^{-1}]	ΔH [kcal mol^{-1}]	ΔS [cal mol^{-1} K]
2	$(1.0\pm0.1)\times10^6$	-8.2 ± 0.1	-7.0 ± 0.1	4.2 ± 0.1
3	$(4.4\pm0.4)\times10^5$	-7.7 ± 0.1	-5.3 ± 0.1	8.2 ± 0.2
4	$(1.6\pm0.1)\times10^6$	-8.5 ± 0.1	-6.7 ± 0.1	6.0 ± 0.1
5	$(3.7\pm0.1)\times10^5$	-7.6 ± 0.1	-4.9 ± 0.1	9.1 ± 0.2
6	$(2.3\pm0.1)\times10^5$	-7.3 ± 0.1	-5.6 ± 0.1	5.9 ± 0.1
7	$(1.7\pm0.1)\times10^5$	-7.1 ± 0.1	-4.6 ± 0.1	8.6 ± 0.2

[a] ITC experiments were conducted at 25 °C in duplicate with the same batch of ligand and Grb2 SH2 domain in 2-[4-(2-hydroxyethyl)piperazin-1-yl]ethanesulfonic acid (HEPES, 50 mM) with NaCl (150 mM)

Aaron P. Benfield, Martin G. Teresk, Hilary R. Plake, John E. DeLorbe, Laura E. Millspaugh, Stephen F. Martin
Angew. Chem. Int. Ed. **2006**, *45*, 6830 –6835

The 55% Rule

Confined Space Occupancy in Apolar Complexation

Molecular Capsules

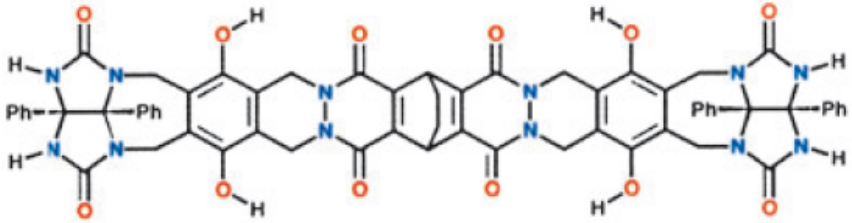

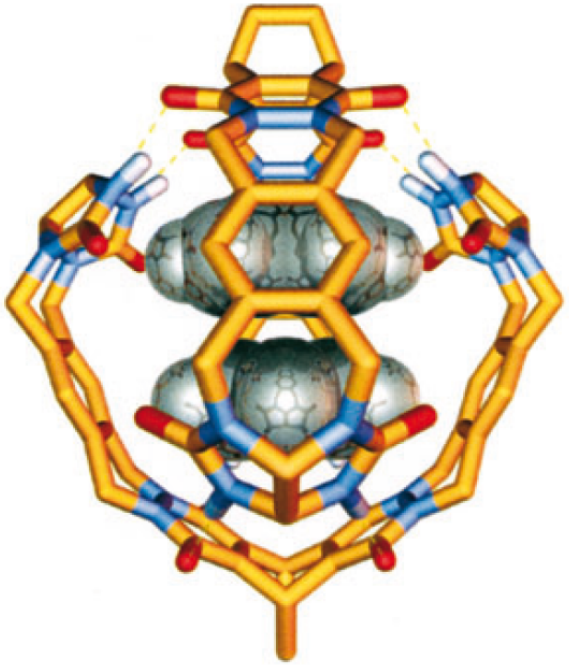

Wyler, de Mendoza, Rebek, Jr., *Angew. Chem. Int. Ed.* **1993**, *32*, 1699.
Kang, Rebek, Jr., *Nature* **1996**, *382*, 239.

The 55% Rule

Confined Space Occupancy in Apolar Complexation

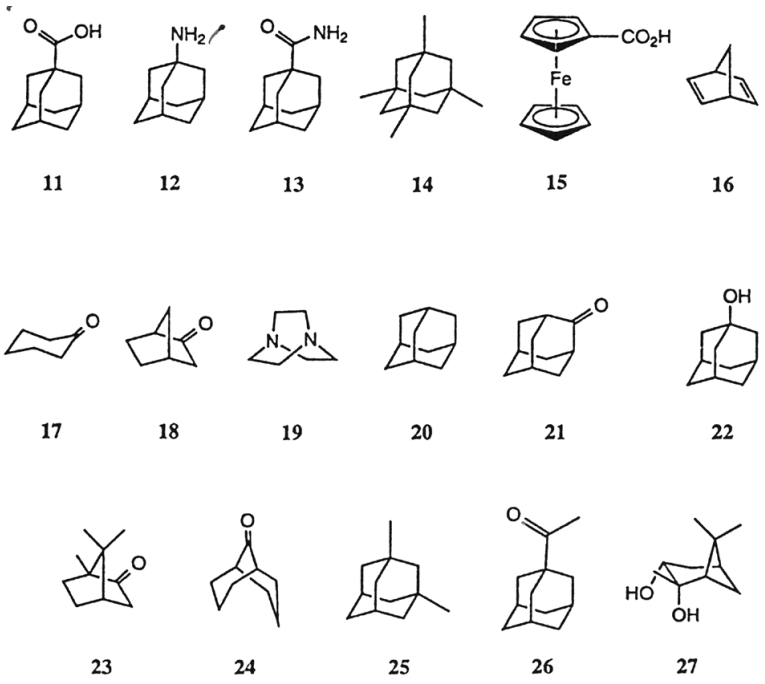

Structures of the guests used in the encapsulation studies.

Binding constants, volume, and packing coefficients for selected guests in capsule **7·7** .

	Binding constant	Volume [Å^3]	Packing coefficient
16	12[a]	97	0.43
17	1700[b]	103	0.46
18	1800[b]	110	0.49
19	500[b]	102	0.45
20	3800[b]	125	0.56
21	5.2×10^5[b]	132	0.59
22	5.2×10^5[b]	135	0.60
23	910[a]	160	0.71
11	130[a]	154	0.68
24	510[b]	142	0.63
25	0	154	0.68
26	0	181	0.80

[a] Measured by direct binding. [b] Measured by competitive binding.

The 55% Rule

The interior of molecular capsules has been utilized to catalyze the Diels-Alder addition, and chiral capsules have been shown to differentiate between guest enantiomers.

In this context, one of the most important findings is the so-called **55%-rule** (S. Mecozzi, J. Rebek, *Chem. Eur. J.* **1998**, *4*, 1016). Studies with a large number of capsules, such as **7·7** (next slide) and a variety of guests indicate **an optimal ratio of guest van der Waals volume and capsule interior volume. A ratio of 55 ± 9% gives optimal binding. Remarkably, this is also the packing density in most organic liquids.**

Smaller guests are disfavored because the interior is becoming desolvated while in addition the guest experiences less enthalpy-lowering contacts as compared to the bulk solvent.

Larger guests are artificially "frozen": A large entropic loss results from the loss of translational and rotational degrees of freedom.

Note that this 55%-rule holds mainly for hydrophobic and van der Waals complexation. Synthetic and biological complexation involving H-bonding and ion pairing, for which the Coulomb law holds, have much higher packing and volume occupancy coefficients.

Applications – Supramolecular Catalysis

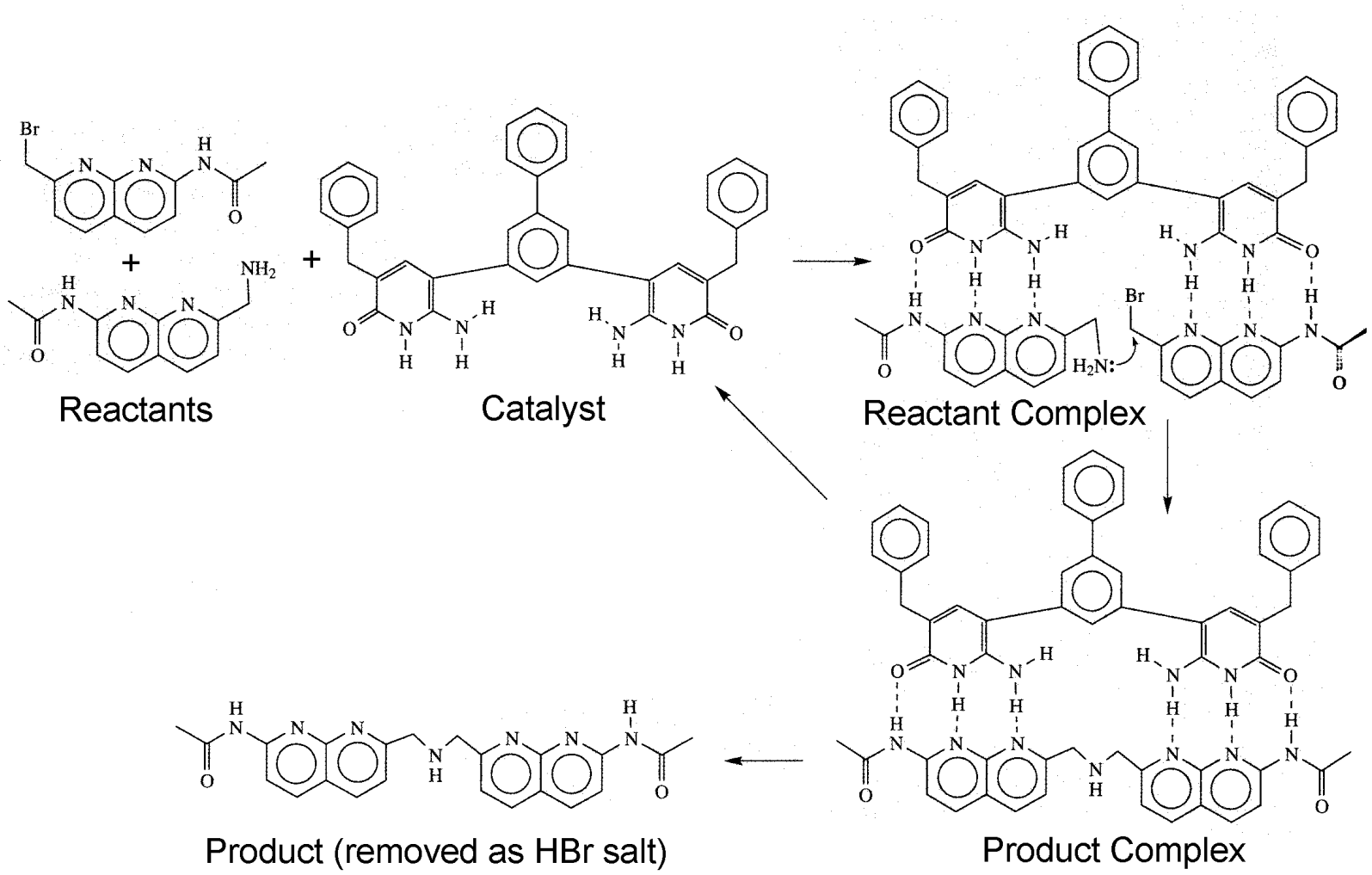

Applications – Cation Transport

Light-driven cation transport with the help of azobis(crownether):

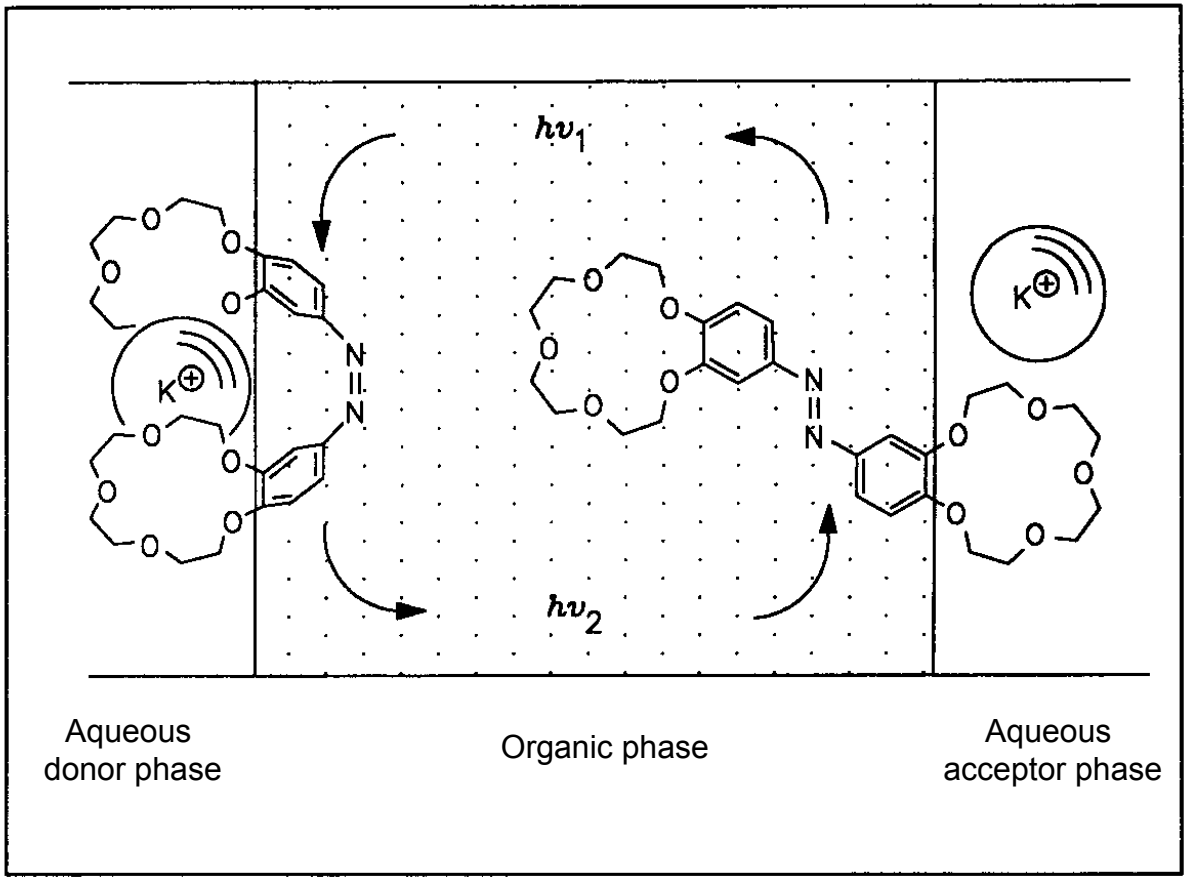

Applications – Molecular Machines

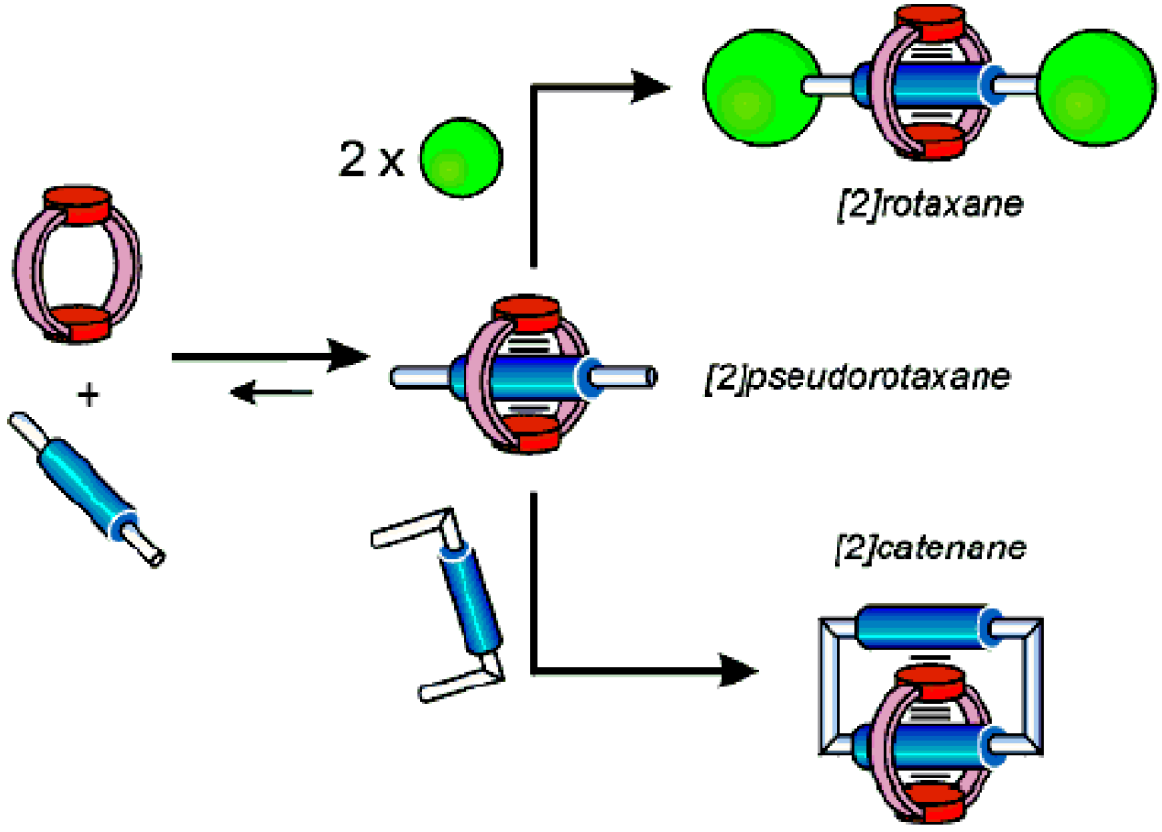

Applications – Rotaxane-Shuttle

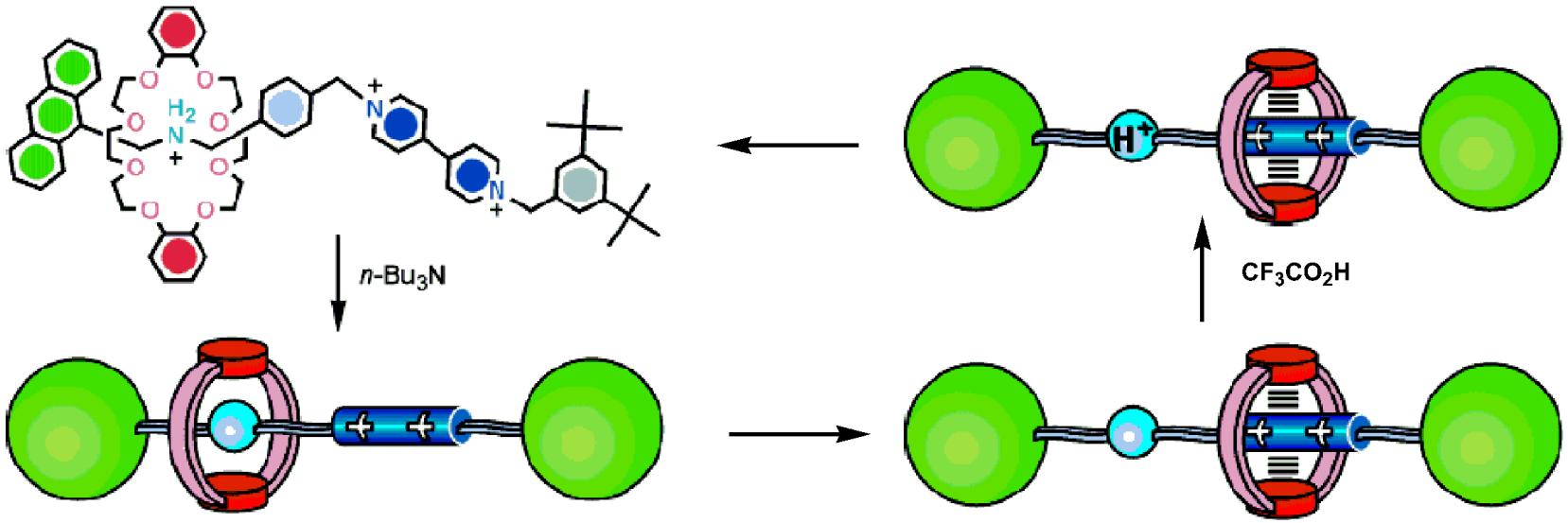

Ein chemisch kontrollierbares molekulares Shuttle: der Ring kann zwischen den beiden “Stationen” der stabförmigen Komponente des Rotaxanes durch Base/ Säurezugabe (MeCN, Raumtemperatur) hin und her geschaltet werden.

Applications – Rotaxane-Shuttle

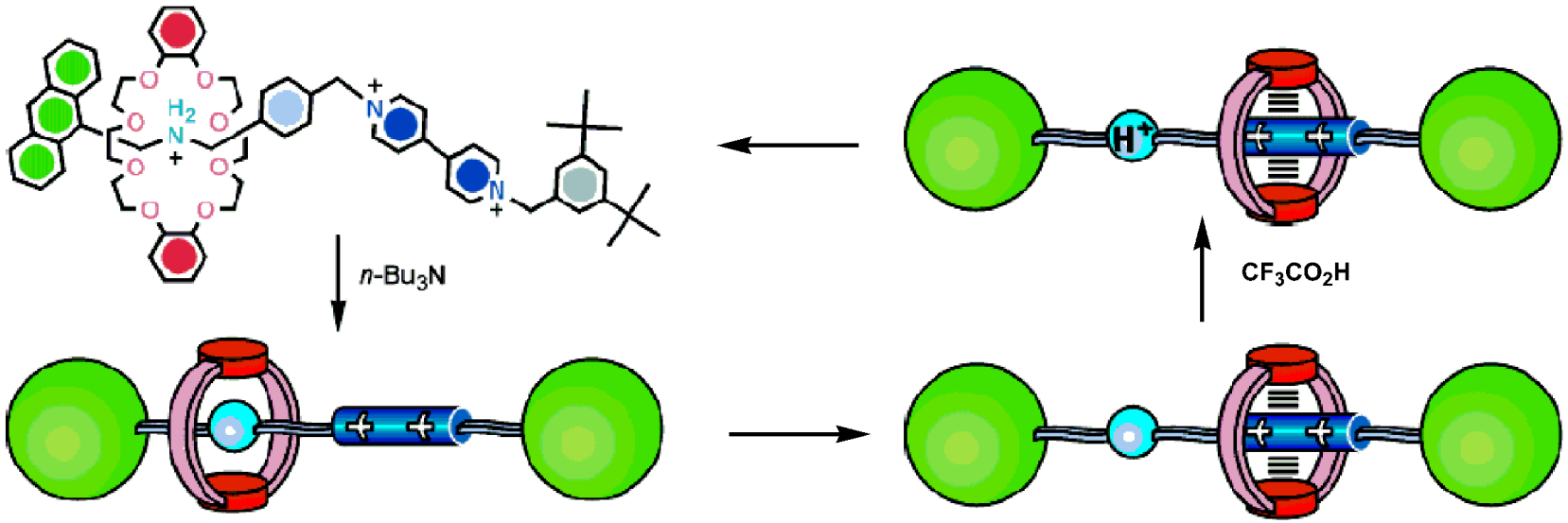

Ein chemisch kontrollierbares molekulares Shuttle: der Ring kann zwischen den beiden “Stationen” der stabförmigen Komponente des Rotaxanes durch Base/ Säurezugabe (MeCN, Raumtemperatur) hin und her geschaltet werden.

Applications – Artificial Muscle